CHARACTERISATION OF MONTMORILLONITE ON POLYVINYL ALCOHOL-STARCH COMPOUND

GOBINATH S/O REHO

A project report submitted in partial fulfilment of the requirements for the award of the degree of Bachelor (Hons.) of Chemical Engineering

Faculty of Engineering and Science
Universiti Tunku Abdul Rahman

April 2012

DECLARATION

I hereby declare that this project report is based on my original work except for citations and quotations which have been duly acknowledged. I also declare that it has not been previously and concurrently submitted for any other degree or award at UTAR or other institutions.

Signature : _____

Name : GOBINATH S/O REHO

ID No. : 08UEB06890

Date : _____

APPROVAL FOR SUBMISSION

I certify that this project report entitled **"CHARACTERISATION OF MONTMORILLONITE ON POLYVINYL ALCOHOL-STARCH COMPOUND"** was prepared by **GOBINATH S/O REHO** has met the required standard for submission in partial fulfilment of the requirements for the award of Bachelor of Engineering (Hons.) Chemical Engineering at Universiti Tunku Abdul Rahman.

Approved by,

Signature : _____

Supervisor : Dr. Lee Tin Sin

Date : _____

ACKNOWLEDGEMENTS

I would like to thank everyone who had contributed to the successful completion of this project. I would like to express my gratitude to my research supervisor, Dr. Lee Tin Sin for his invaluable advice, guidance and his enormous patience throughout the development of the research. Besides, I would also like to thank my research co-supervisor, Ms. Bee Soo Tueen for her initiative to guide me throughout this research.

In addition, I would also like to express my gratitude to my loving parent and friends who had helped and given me encouragement in terms of moral and financial in completing this research successfully.

CHARACTERISATION OF MONTMORILLONITE ON POLYVINYL ALCOHOL-STARCH COMPOUND

ABSTRACT

Polyvinyl alcohol (PVOH) and polysaccharide (starch) are widely used in biodegradable plastic packaging application and in few other fields. Since different polarities of starch present some drawbacks, nano-sized montmorillonite (MMT) was used as a reinforcing material for both polyvinyl alcohol and starch blend in this research. Three compounds (PVOH-MMT- corn starch) were blended together, cast and was analysed. Amount of montmorillonite incorporated was varied from 0.1 g to 0.9 g and amount of PVOH was varied from 20 % to 100 %. Characterisation was made according to their mechanical properties, thermal properties, morphologies, and interaction of bonding. Mechanical properties were seen to increase for a certain level of MMT incorporation up to 0.5 g for sample with neat PVOH. MMT loadings up to 0.9 g with 50 % of PVOH possess even better mechanical properties. DSC results showed that the highest enthalpy of melting of 59.56 J/g was achieved with the addition of 0.5 g MMT in the neat PVOH sample. FTIR analysis showed that the interaction of bonding between the molecules was strongest when 0.9 g of MMT was incorporated with 50 % of PVOH. SEM images suggested that the MMT particles were well distributed when 0.5 g of PVOH was incorporated with 100 % PVOH. A better and tinier distribution was observed for samples containing 0.9 g MMT and 50 % of PVOH. In short, addition of MMT only up to 0.5 g in 50 % of PVOH possesses the highest mechanical properties and addition of 0.9 g MMT into 50 % PVOH possesses strongest interaction of bonding between molecules. Moreover, addition of MMT only up to 0.5 g in neat PVOH possesses highest thermal stability.

TABLE OF CONTENTS

LIST OF TABLES

LIST OF FIGURES

LIST OF SYMBOLS / ABBREVIATIONS

c_p	specific heat capacity, J/(kg·K)
h	height, m
P	pressure, kPa
P_b	back pressure, kPa
R	mass flow rate ratio
T_g	glass transition temperature
T_m	melting temperature
α	alpha
β	beta
ρ	density, kg/m^3
wt %	percentage of weight
ΔH_m	enthalpy of melting, J/g
CRS	Corn Starch
PVOH	Polyvinyl Alcohol
MMT	Montmorillonite

LIST OF APPENDICES

CHAPTER 1

INTRODUCTION

1.1 Background

Biodegradable polymers are polymer that is designed to degrade upon disposal by the activity of living microorganism. Biodegradable plastics are either produced from naturally renewable polymers or synthetic polymers. Since synthetic polymers are derivation of petroleum, they are considered expensive. On the other point of view, natural polymers are considered as inexpensive. However, natural polymers are limited in their ability to obtain wide commercial application due to disadvantages in mechanical properties and brittleness. However, the weakness of biopolymer films in mechanical properties may not be easily overcome.

Polyvinyl alcohol (PVOH) is well known as a biodegradable synthetic polymer. It is produced through the hydrolysis of polyvinyl acetate. Polyvinyl alcohol is non toxic, strong, durable, highly crystalline, water-soluble polymer and has good film-forming and high hydrophilic properties (Elzawawe & Nassar, 2010). PVOH is consumed by microorganisms and enzymes when it is exposed to natural environment (Chiellini, Corti, & Solaro, 1999; Spiridon, Popescu, Bodarlau, & Vasile, 2008). PVOH is certainly suitable for biodegradable packaging applications. Besides, PVOH can also be used in biomedical fields as biocompatible tissue scaffolding materials to increase growth of transplanted cell and it degrades after the formation of new tissues (Sinha, Bandyopadhyay, & Bousmina, 2007).

Moreover, PVOH do play important role in pharmaceutical fields where it has the ability in transporting drugs and bioactive agents (Constantin, Fundueanu, Bortolotti, Cortesi, Ascenzi, & Menegatti, 2004). Since polyvinyl alcohol became important in variety of applications, the price of PVOH hikes making it to be an expensive polymer. Economically, to reduce the cost of producing biodegradable plastics, researchers have found that blending of PVOH and starch is a favourable method (Chen, 1997; Cinelli, 2002; Gordon, 2002; Imam, 2002; Liu, 1999).

Polysaccharide or starch is one of the main natural polymers used in production of biodegradable materials. It is the most abundant macromolecules in the biosphere. Starches are derived from natural sources like rice, maize, potatoes, cassava and pea. Researches have introduced starch in biodegradable polymer production because of its renewability, biodegradability, wide availability and low cost (Huang, 2005; Ma & Yu, 2007; Tang & Zou, 2008; Thakore, Desai, Sarawade, & Devi, 2001). As mentioned, blending of PVOH and starch compound is economically beneficial because both of the compounds are polar substances which having hydroxyl group (-OH) in their chemical structures (Chen, 1997; Cinelli et al., 2002; Liu, 1999; Siddaramaiah & Baldev, 2003). These tend to form strong intermolecular hydrogen bonds that improve the integrity of PVOH-starch blends (He, Zhu & Inoue, 2004; Rahmat, Rahman, Lee, & Yussuf, 2009). The blending of synthetic polymer and starch increases biodegradability. However, different polarities of starch present some drawbacks, such as the strong hydrophilic behaviour and poorer mechanical, barrier and thermal characteristics (Park & Yoon, 2005; Tang & Xiong, 2008; Thakore, 2001).

Experimental investigations have shown that polymer/layered silicate nanocomposite films can improve the mechanical, barrier, thermal and moisture adsorption properties of packaging material (Kaczmarek, & Podgorski, 2007). To improve the mechanical and barrier properties of starch composite at the same time, certain amount of inorganic is normally added to a polymer matrix. Montmorillonite (MMT) is one of the most widely used types of smectite clay in polymer nanocomposites nanofillers. Montmorillonite is smectite clay with layered structure. It is a reinforcing material, naturally abundant, non toxic, inexpensive, chemically and thermally stable.

Special attention has been also paid to montmorillonite minerals because of their small, extremely large surface areas and intercalation properties. Montmorillonite is composed of silicate layers that are 1 nm thick in planar structure and 200-300 nm in the lateral dimension (Piyaporn, Duangdao, Duanghathai & Kawee, 2007). MMT can be used as one of the components for food packaging, medical, cosmetic and healthcare recipients (Rao, 2007).

1.2 Problem Statements

Polyvinyl alcohol and starch blend is considered as a biodegradable polymer used in biodegradable packaging application, biomedical fields as biocompatible tissue scaffolding materials to increase growth of transplanted cell and pharmaceutical fields where it has the ability in transporting drugs and bioactive agents. Polyvinyl alcohol has plenty of biodegradable natures. However, PVOH is quite expensive in price. To overcome this economical issue, researchers found that blending starch together with PVOH is favourable (Chen, 1997; Liu, 1999; Cinelli et al., 2002). However, it is also found that different polarities of starch would deteriorate the existing mechanical properties of PVOH. Hence, this research is done to evaluate the effect of montmorillonite (MMT) as it is added to PVOH-starch compound. Following are the problem statement for this study:

1. What are the mechanical properties and thermal properties as montmorillonite was incorporated into PVOH-starch blend?
2. How do the surface morphologies change and the interaction of bonding between the blended compounds as montmorillonite was incorporated into PVOH-starch blend?

1.3 Aims and Objectives

The aim of this study was mainly to evaluate the characteristics of the polyvinyl alcohol-starch compound and their corresponding interactions with montmorillonite components for further explore its application in wide range of industry. The best possible amount of polyvinyl alcohol, starch and montmorillonite compound in the blend was investigated. The main objective was divided into sub objectives such as:

1. To evaluate the mechanical properties and thermal properties of the blend.
2. To observe the surface morphologies and to evaluate the bonding interactions such as chemical features and shifts of the blend.

1.4 Scope of study

This study described the characterisation of the polyvinyl alcohol-starch compound when montmorillonite (MMT) was blended in together. A film composite of the polyvinyl alcohol, starch and montmorillonite was obtained. Several characterisation techniques were applied to characterise the blend film composite of montmorillonite in polyvinyl alcohol-starch compound.

1.4.1 Mechanical Properties

Tensile test was done to measure the force required to break the blended specimen and the extent to which the blended specimen stretches or elongates to its breaking point. From the tensile test, a stress-strain diagram was produced and was used to determine the tensile strength, percentage elongation at break and its modulus. The blended film was tested according to ASTM D882 standard.

1.4.2 Thermal Properties

The onset, endpoint melting temperature and the enthalpy of melting was obtained from the Differential Scanning Calorimetry (DSC) analysis.

1.4.3 Physical Properties/ Morphologies

The surface of films after incorporating with montmorillonite was examined for changes in its phase morphology using Scanning Electron Microscopy (SEM).

1.4.4 Interactions of bonding

Fourier Transform Infrared (FTIR) was used in this study to identify chemical features and shifts that occur due to the interactions between functional groups of the blended specimen. FTIR generates an infrared spectral scan of sample that absorbs infrared light.

CHAPTER 2

LITERATURE REVIEW

2.1 Mineral type of additives

According to Mohod and Gogate (2010), PVOH is one of the most important and commonly used polymer with uses as adhesive and thickener material in things like paints, detergent and so on. In United States of America, the US Food and Drug Administration allows polyvinyl alcohol for use as an indirect food additive in products that are in contact with food. In addition to food-contact use, polyvinyl alcohol is approved as diluents in colour additive mixtures for colouring shell eggs. Polyvinyl alcohol is used in FDA- approved drug products for use in several medical applications, including transdermal patches, the preparation of jellies that dry rapidly when applied to the skin, and in immediate and sustained release tablet formulations.

Polyvinyl alcohol is also used is as an ophthalmic demulcent at 0.1–4.0% compositions (Kelly, DeMerlis, Schoneker, & Borzelleca, 2003). Polyvinyl alcohol is included in the FDA Inactive Ingredient Guide (IIG) for ophthalmic preparations and oral tablets. In order to enhance the biodegradation rate and lower the cost of polyvinyl alcohol lies in preparing composites with more biodegradable, cheaper, and easily processed fillers or polymers.

PVOH based biodegradable composites have been prepared by few researchers by incorporating it with different types of natural polymers such as starch (Siddaramaiah, Raj, & Somashekar, 2004), soy protein (Su, Huang, Liu, Fu, & Liu, 2007), cellulose (Ramaraj, 2006), chitin and chitosan (Jia, Gong, Gu, Kim, Dong, & Shen, 2007), and so on. Figure 2.1 below shows an example of the possible hydrogen bond between starch and PVOH.

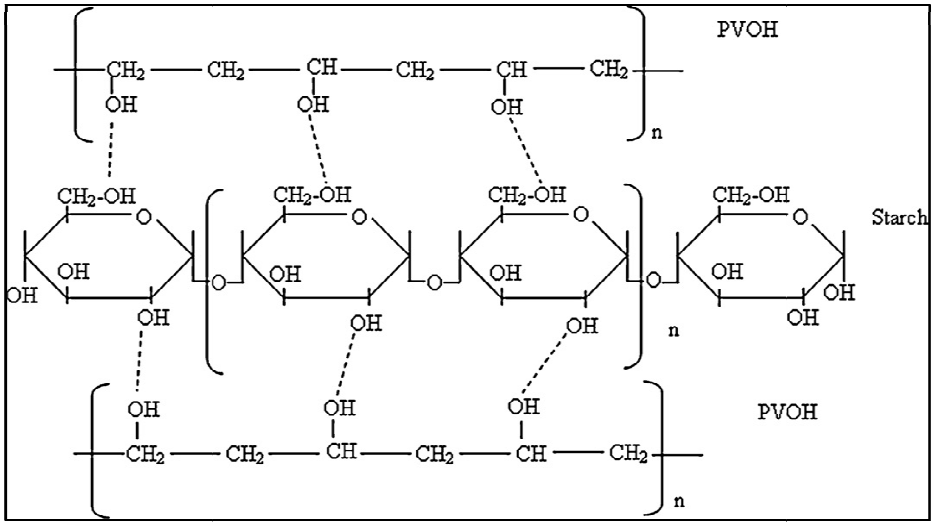

Figure 2.1: Possible Hydrogen Bond between Starch and PVOH (Tang & Alavi, 2011)

Mineral types of additives are also common in biodegradation process. Mineral types of additives such as hematite and zerovalent iron are often used as remediation of soils contaminated with inorganic pollutant such as chromate copper arsenate (CCA) (Hartley, Edwards, & Lepp, 2004). Iron hydroxides can be effective sorbents for both anions and cations since the surface of hydroxide particles can be positively or negatively charged depending on pH making the iron hydroxides amphoteric. Natural zeolites, such as alumino-silicate mineral can be effective since they have certain characteristics such as strong capability of ion exchange, large surface area and adsorption for their particular tetrahedral pore framework.

On the other hand, they are considered one of the cheapest and abundant materials, which have also been utilised as adsorbent for removal of metals (Babel & Kurniawan, 2003; Kocaoba, Orhan, & Akyuz, 2007; Panuccio, Crea, Sorgona, & Cacco, 2008; Gupta & Rastogi, 2008). Clay minerals are a categorised as phyllosilicates which are normally known as an outcome of chemical weathering of other silicate minerals on the earth surface. Montmorillonite, hectorite, fluorohectorite and saponite are the most commonly used clay minerals for the preparation of polymer nanocomposites taking advantage of their delamination of clay minerals (Mihai, Pauly, & Pinnavaia 2000; Zhou, 2010).

Researchers have shown that adding a small amount of these clay minerals (5-10 wt %), with a certain degree of exfoliated structure, give tremendous influence on the properties of the final material. Properties such as thermal stability, mechanical strength, stiffness, conductivity and gas barrier properties are obviously influenced by the addition of clay minerals (Ray & Okamoto, 2003; Ray & Bousmina, 2005; Tjong, 2006; Xiong, Zheng, Jiang, Ye, & Wang, 2007).

The nanocomposite structure depends on the clay mineral polymer compatibility and also on the processing conditions (Avella, Bondioli, Dipace, Errico, Ferrari, Focher, & Malinconico, 2006; Fornes, Yoon, & Paul, 2003; Hablot, Bordes, Pollet, & Averous, 2008; Homminga, Goderis, Hoffman, Reynaers, & Groeninckx, 2005 Zenggang, Chixiang, & Na, 2002). It is believed that the properties are related to high aspect ratio of exfoliated structure (Alexandre & Dubois, 2000). The hydrophilic nature of montmorillonite limits its compatibility with certain polymers for example organophilic polymers. Thus, chemical modification is done to develop the compatibility. Figure 2.2 below shows the 3D crystal image of pure MMT. As a chemical modification, montmorillonite is incorporated with alkylammonium salts to form organo-montmorillonite (OMMT). Although montmorillonite is abundant, this naturally occurring mineral always contains impurities that can affect some catalytic properties. For hectorite, although it is relatively scarce in natural deposits, it can be prepared by hydrothermal reaction (Zhou, Du, Li, Lu, & Ge, 2005).

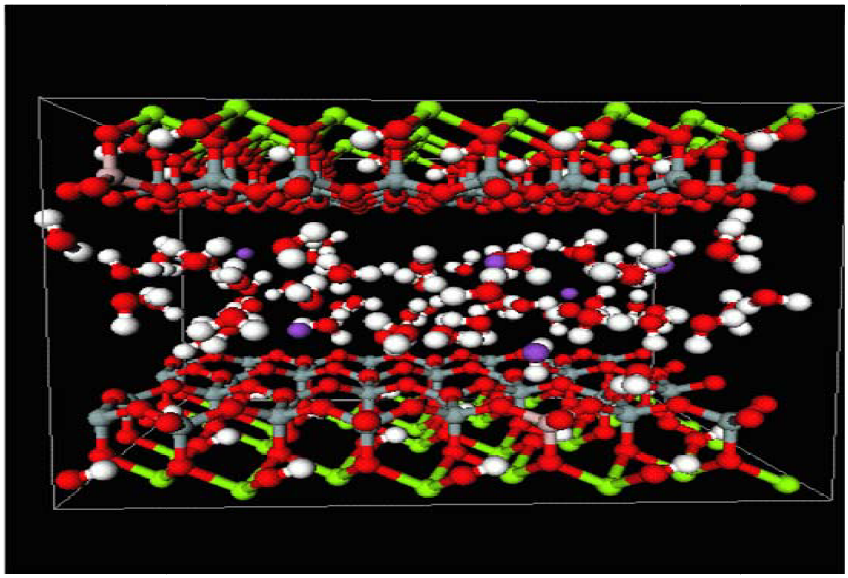

Figure 2.2: Three Dimensional (3D) crystal image of montmorillonite (Ray & Bousmina, 2005)

According to Zhang, Tong, Xia, Jiang, Liu, Yu, and Zhou (2009), synthetic clay minerals with a good designed composition and structure gives advanced functional materials for new applications which require homogeneous samples. Thus, the synthetic clay minerals are important industrially and academically. Synthetic kaolinites form under three conditions which are chemical weathering, hydothermal alterations and sedimentar rock. All process occurs at low temperature by alteration of primary minerals such as feldspars, albite and muscovite (Murray, 1988).

Hydrothermal synthesis of kaolinite-like solids yields better product compared to low temperature synthesis. For synthetic pyrophyllites there are actually three polytypic forms which are 2-layer monoclinic (2 M), 1-layer triclinic (1Tc) and disordered form that are often associated and intergrown (Bruno, Prencipe, & Valdre, 2006). As for synthetic mica, the composition, pureness, particle size and layer charge of synthetic micas can be controlled during synthesis and fitted to specific uses. For example, organo-fluorophlogopites were of higher purity and better reproducibility than those from natural montmorillonite (Baldassari, Komarneni, Mariani, & Villa, 2006).

Egyptian bentonite (EB) is commonly used to build viscosity quickly and to support bore-hole walls for preventing collapse and sloughing. Studies on its beneficiation and applications (Hassan & Khalek, 1998) and the influence of polyacrylamide addition on its rheological properties (Mostafa, Assaad, & Attia, 2007) report its possible uses especially as drillingmud. Turkish commercial zeolite (TZ) contains N90% clinoptilolite / heulandite (Saltali, Sari, & Ayidin, 2007). Zeolites are known for their relatively large cation exchange capacity (CEC) when compared with smectites and for their channels that lead to permanent porosity. Other than that, they have a three dimensional network of interconnected pores compared to others. It is used as soil conditioner, to improve physical and chemical properties and remove hazardous chemicals.

Research have also showed that, zeolites are applicable in the process of removing ammonium from effluents was emphasized (Karadag, Koc, Turan, & Armagan, 2006). Pure-Flo B80 (PF) is defined by the distributor as an intergrowth of smectites and minerals from the palygorskite/sepiolite group, and is suggested for the use in removing colour and chlorophyll from liquids. Other than that, it could also been use for removing detergents from effluents. Moreover, several studies also used it for oil refining and pre-treatment (Antoniassi, Esteves, & Meirelles, 1998), and for removing or avoiding the presence of iodine (Jain & Proctor, 2007). Calcium carbonate is another type of common and widely used filler for many industrial applications such as plastics, papermaking and rubber. Medically, calcium carbonate has been known as the bone filling material due to its good osteo-conductivity (Fujihara, Kotaki, & Ramakrishna, 2005), slow biodegradability and easy production (Ishikawa, Murano, Hiraishi, Yamaguchi, Tamai, & Tsuji, 2002). Since there is no layered structure in calcium carbonate, neither intercalation nor exfoliation occurs in its enzyme composite. However, it still has the capability to entrapped enzymes via physical adsorption as it has large interfacial area in calcium carbonate aggregates. Nanosized calcium carbonate has greater advantages and novel characteristics than regular sized particles, such as the much larger specific surface area and the tendency to aggregate. These properties constitute favourable conditions for enzyme

immobilization. Nevertheless, to our knowledge, calcium carbonate nanoparticles have never been used for the construction of a biosensor.

According to Davidovits (1994), aluminosilicate powders including natural pozzolans can synthesize geopolymers that is to come to existence by co-polymerization with higher pH of alkaline. Research shows that natural pozzolans from Iran has good potential as a source of aluminosilicate (Bondar, 2009). Previous work has shown that factors such as increasing molar Si–Al ratio and % CaO have positive effects on the final compressive strength of geopolymer cement (Xu & Van Deventer, 2000). The aluminosilicate used for the production of a geopolymer cement must contain aluminium which is readily soluble with an overall molar ratio of Al_2O_3:SiO_2 (1:3.3 to 1:6.5) between (Van Jaarveld, Van Deventer, & Lorenzen, 1997). According to the researchers, the ratio is just an approximate composition because they are actually based on chemical analysis. Often the rate of dissolution of Al from natural aluminosilicates is insufficient to produce a gel of desired composition (Xu & Van Deventer, 2000). To synthesize geopolymers, kaolinite is also used as secondary source of soluble silicon and aluminium because it is considered as inexpensive. Longer setting time of desired gel composition could be produce as the exact amount of kaolinite is added to the natural aluminosilicates. However, if kaolinite on its own is used without the presence of other natural minerals, a weak structure is formed (Xu et al., 2000).

Other than that, the amount calcium should also be taken into account as it does affect the setting time and the properties of geopolymers (Xu et al., 2000). Thus, exact amount of CaO should be added to the natural aluminosilacte to increase the overall strength of natural pozzolan. Natural pozzolans are geological deposits with a wide range of chemical compositions which vary from batch to batch but they are usually high in available SiO_2. Deficiencies in the SiO_2, Al_2O_3 and CaO content in a natural pozzolan might be compensated for by adding. Blending of polyvinyl alcohol and montmorillonite has been reported in a number of studies to determine their suitability for a range of practical applications, such as wound dressings (Kokabi et al., 2007). Both polyvinyl alcohol and montmorillonite are hydrophilic and the incorporation of the smectite clay into the polymer can be achieved via a relatively easy dispersion process.

A method called solution intercalation method is one of the ways of preparing PVOH-MMT composites. This method is actually based on the capability of silicate swelling and utilisation of a solvent that polymer is soluble. Figure 2.3 below shows the morphology of pure smectite montmorillonite clay under Scanning Electron Microscopy (SEM).

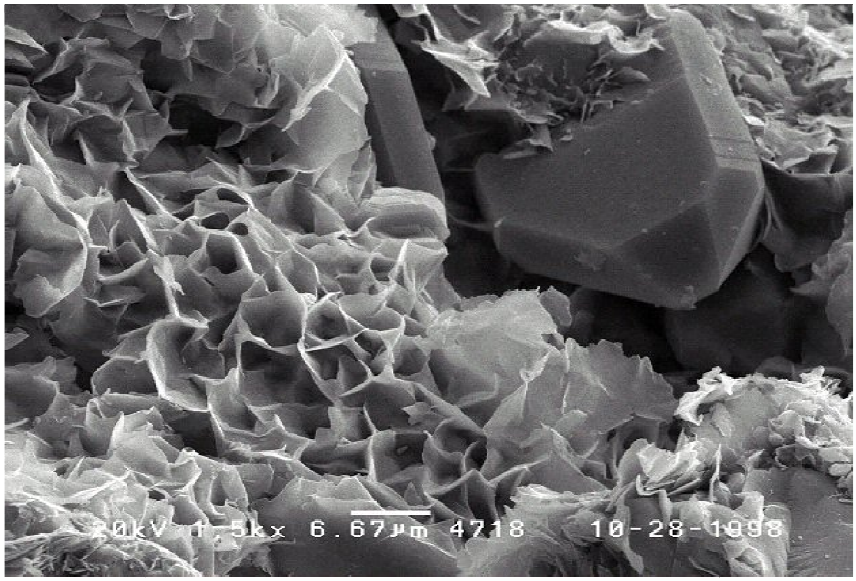

Figure 2.3: Rosette morphology of pure smectite montmorillonite clay (OMNI Laboratories Inc, 1998)

In a study, by using ESEM, for micrographs of PVOH-MMT (70:30) the clay particles are agglomerated and exfoliation was not achieved. For PVOH-MMT (50:50) the clay layers are not separated by the polymer to form neither intercalated nor exfoliated composites and there were no changes even when the sonication time increased. The clay particles re-aggregated into larger clusters and could not be separated by shaking for PVOH-MMT (90:10).

The effects of the montmorillonite concentration in polyvinyl alcohol were shown clearly in scanning electron microscopy (Figure 2.4). With 5 % of montmorillonite (a), the micrograph has some bright dots because of the presence of montmorillonite. With 15 % of montmorillonite (b), there have some bright dots with many of those diffuse dots. As for 40 % of montmorillonite (c) most of the surface becomes white with some very bright dots. According to the researcher, the PVA succeeds in intercalate and exfoliated the montmorillonite to produce a nanocomposite even at high montmorillonite clay content.

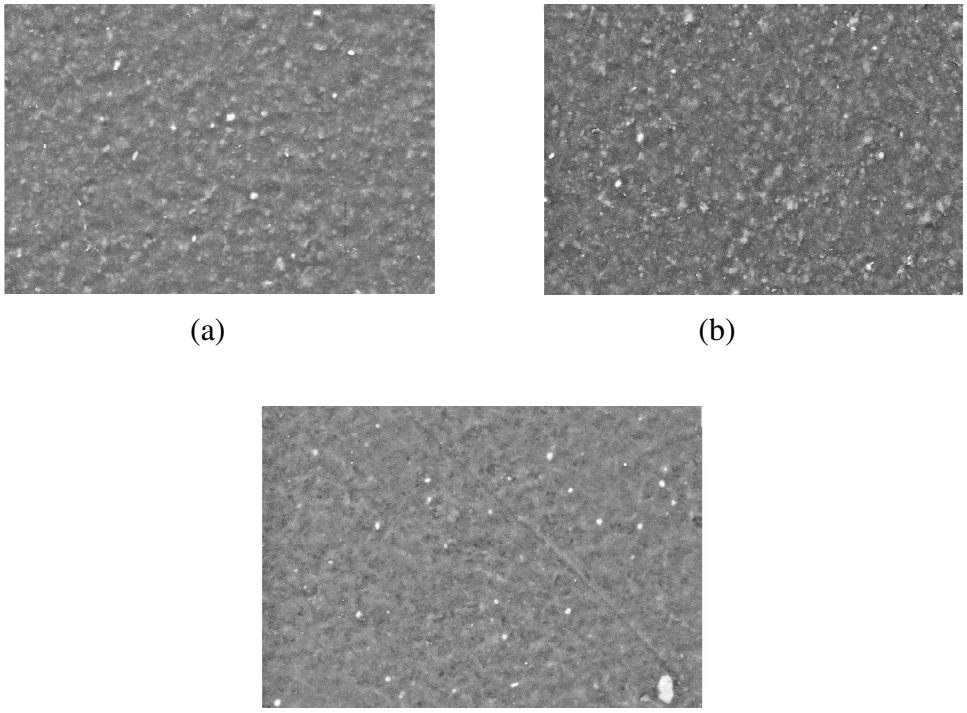

(a) (b)

(c)

Figure 2.4: (a) 5 % MMT; (b) 15 % MMT; (c) 40 % MMT (Cerda, Luengas, Navarrete, Sanchez, & Guzman, 2003)

2.2 Thermogravimetric Analysis of polymer with nanoccomposite

Thermogravimetric Analysis measurements have shown that polymer with nanocomposite has greater thermal stability compared to a pure or virgin polymer. (Chrissafis, Antoniadis, Paraskevopoulos, Vassiliou, & Bikiaris, 2007) have used in situ ring-opening polymerisation of F-caprolactone to prepare nanocomposites with multiwalled carbon nanotubes, fumed silica, as well as with unmodified Cloisite Na^+ and modified Cloisite 20A montmorillonite. According to the researcher, there was a substantial increase in both tensile strength and Young's modulus for the entire nanocomposite but as it comes to thermal stability, only nanocomposite with carbon nanotubes and unmodified montmorillonite showed improved qualities.

Costache, Heidecker, Manias, Camino, Frache, Beyer, Gupta, and Wilkie (2007) have studied the thermal degradation of polyethylene, ethylene-vinyl acetate copolymer and polystyrene nanocomposites with single and multiwall carbon nanotubes, organically modified montmorillonites and layered double hydroxides. As s a result, they found that there were no differences in the degradation products when carbon nanotubes are used but the relative amount of the degradation product are changed when cationic and anionic clays were used. Addition of silica is said to improve the thermal stability of the natural rubber as seen in an increase of both degradation temperature and activation energy of degradation (Li, Yu & Yang, 2005). A Quite similar effect was also observed for silica-polyvinyl alcohol nanocomposites (Peng, Kong, Li, & Spiridonov, 2006).

Kandare, Deng, Wang, and Hossenlopp (2006) found and increase in both the degradation temperature and the activation energy of the degradation for polymethyl methacrylate-layered copper hydroxyl methacrylate composites. Dzunuzovic, Jeremic, and Nedeljkovic (2007) have used a nanocomposite from in-situ radical polymerization of methyl methacrylate in a solution of surface modified TiO_2 nanoparticles. There were no changes reported for its glass transition temperature; however the thermal stability was determined to increase. Products and larger values of the activation similarly,

According to Avella, Carfagna, Cerruti, Ericco, and Gentile (2006), the addition of fatty acid coated calcium carbonate nanoparticles to nylon 6 decreases both the degradation temperature and the activation energy of degradation of the polymer. A Thermal gravimetic analysis study by Krkljes, Marinovic, Kacarevic, and Nedeljkovic (2007) using gamma radiolytically synthesized Ag-PVA nanocomposites have shown that a two-step degradation mechanism was observed at fewer loads of Ag changes to a single-step as the load increases. An effect of nanoconfinement on degradation and relaxation of two structurally different polystyrene–montmorillonite clay nanocomposites was investigated by Chen, Wilkie, and Vyazovkin (2007) and the report showed that the materials of intercalated and exfoliated brush structures presented a high yield of α-methylstyrene in the degradation products and higher value of activation energy for thermal degradation. However, the size of cooperatively rearranging region at the glass transition has been found to be structure dependent, being larger in the exfoliated brush system. The increase or enhancement in both the systems are linked to intermolecular nanoconfinement such as founding of isotactic polystyrene that degrades at higher temperature than atactic polystyrene. The consequences can be brought down to the hindered molecular that manifests itself particularly in the fact that the activation energy of the glass transition is higher for isotactic than atactic polystyrene (Chen et al., 2007).

Dielectric relaxation spectroscopy was applied by Bras, Viciosa, Wang, Dionisio, and Mano (2006) to probe the effect of nanoconfinement by the crystalline phase on crystallization of polylactic acid from the glassy and melt states. Incorporation with regular α– and β– relaxation processes, the earlier stages of the crystallization are followed by the presence of a peak due to the constrained α-process was reported by them. Researchers Saiter, Couderc, and Grenet (2007), have characterized the structural relaxation phenomena of poly (ethylene terephthalate) glycol-montmorillonite nanocomposite containing 1 to 5 wt% of the clay by using regular and modulated DSC. Following the corporation, the value of dynamic fragility, activation energy and the size of the cooperative rearranging region pass through a minimum for the composite containing 3% of montmorillonite.

Koh, McKenna, and Simon (2006), have measured the absolute heat capacity and glass transition temperature of unsupported ultra thin films of polystyrene and the glass transition temperature and the absolute heat capacity in both the glass and liquid states decreased with decreasing the thickness of film thickness reported. Takegawa, Fukao, and Saruyama (2007), have made use of simultaneous measurement of the complex thermal expansion coefficient and the complex heat capacity to study the aging effect on the thermal expansion coefficient and the heat capacity of glassy polystyrene. In all tested cases, it has been shown that the step wise change in the real part of the complex thermal expansion coefficient and the peak of the imaginary part occur at the low temperature than those of the complex heat capacity. Montserrat, Calventus, and Hutchinson (2006) studied the enthalpy relaxation kinetics of several thermosetting powder coatings in order to compare the relative stabilities of alternative to the triglycidyl isocyanurate system. Eventually, the outcome has shown that in the triglycidyl isocyanurate coatings the aging rate is slowest.

The thermal degradation of cellulose is essentially similar in both air and nitrogen; this was confirmed by Mamleev, Bourbigot, and Yvon (2007) with modulate TGA measurements. The two phase modal of cellulose is proposed to explain all observable phenomena related to its pyrolysis in inert and oxidative atmospheres. A research by Erikson (2007) combining DSC ,TGA and evolved gas analysis has established a common set of chain scission mechanism involving the aromatic moieties in polyurethane, epoxy, poly(Diallylphthalate), polycarbonate and poly(phenylene sulfide). Suleiman, Napadensky, Sloan, and Crawford (2007) who have employed TGA to identify the effects of sulfonation (53-97%) and counterion (Mg^{2+}, Ca^{2+}, $Ba2^{+}$) substitution on the thermal stability of block copolymers poly (styrene -isobutylene - styrene) found that due to breakage of sulfonate linkages, sulfonated samples degrades at approximately 300 ºC. These employment however did not occur in the counterion neutralise polymers that start degrading at approximately 450 ºC. Aracil, Font, Conesa, and Fullana (2007) have analysed the thermal degradation of polychloroprene in inert and oxidative atmospheres by using TGA and mass spectrometry to propose reaction modals for pyrolysis and combustion of the polymer.

Tidjani and Wilkie (2006) have employed TGA to test the effect of γ – radiation on the thermal degradation of low - density polyethylene. They report that an outcome of the composition between cross linking and scission caused by irradiation depends on the presents of oxygen, so that an enhancement of the thermal stability does not occurs in samples irradiated in air but occurs in samples irradiated under vacuum. In another study of thermal degradation of polypropylene on Al-MCM-41, it was proposed to use model-free values of activation energy obtained for systems with different amounts of catalyst as a criterion for finding the optimum amount (Saha & Ghoshal, 2007). Braun et al. (2006) have analyzed the influence of the oxidation state of phosphorus on the decomposition and fire behaviour of flame-retarded epoxy resin that contain approximately 26% of phosphorus in the form of phosphate, phosphonate, phosphinate, and phosphine oxide. As a conclusion, increasing the oxidation state of phosphorus leads to increase in thermally stable residue and decrease in the release of phosphorus-containing volatiles. A report by Howell (2007) has shown that the results of thermal characterization of dual-functional flame retardants that are active both in gas and condensed phase.

Howell and Uzibor (2006) have proposed to enhance fire resistance of poly (styrene) by combining a flame retardant structural unit directly into the main chain that have been accomplished by using an initiator 2,4,5,5-pentaphenyl-1,3,2-dioxaphospholane for styrene polymerization. Thermal gravimetric analysis showed that the thermal stability of the resulting polymer is similar to poly (styrene) generated by conventional methods. Silvestre, Cimmino, Duraccio, and Schick (2007) have observed that the complete crystallization curve ranging from T_g to T_m has a bimodal form for both iPP and iPP-HR blend by applying superfast and regular calorimetry which helps to look at the isothermal crystallization isotactic poly (propylene) and isotactic poly(propylene)-hydrogenated hydrocarbon resin blend. Perrin, Nguyen, and Vernet (2007) found that there were no reasonable kinetics parameters for Horie's mechanistic model but by using a model-free approach, it allowed for reliable kinetic predictions.

Hargis, Grady, Aktas, Bomireddy, Howsman, Altan, Rose, and Rose (2006) have measured the heat flow by DSC and storage modulus by rheometry to monitor the fractional conversion of epoxy curing. The difference was obviously different for both DSC and rheometry. The temperature dependence of the rheological gel times yielded activation energies of curing that have been generally consistent with those derived DSC data. Boz, Nemeth, Ghiviriga, Jeon, Alamo, and Wagener (2007) studied a series of precision ethylene-vinyl chloride polymers via condensation polymerization. According to TGA runs, these polymers have higher stability to thermal loss of HCl compared to PVC. DSC data showed an increase in the temperature and enthalpy of melting that indicates an increase in the degree of disorder associated with introducing the chlorine atoms into the crystalline lattice. The odd numbered polyesters demonstrate two liquid crystalline phase transitions, whereas three transitions are observed in the even numbered systems when odd-numbered main chain polyesters were made (Jeong, Knapp, Ge, Graham, Tu, Leng, Xiong, Harris, & Cheng, 2006).

Fukushima, Drzal, Rook, and Rich (2006) have developed a procedure for exfoliating graphite flakes that has been utilised for the production of nylon and high density polypropylene nanocomposites. On the basis of the results of DSC and other measurements, it is reported that the addition off a small amount of exfoliated graphite flakes showed an improvement thermally. Jaffe, Collins, and Menczel (2006) discussed the intricacies of the thermal analysis of fibres, whose behaviour always reflects the entire history of the fibre, from the synthesis through storage environment prior to sampling. Hatakeyama, Onishi, Endo, and Hatakeyama (2007) have looked at the effect of molecular weight on the thermal gelation of methylcellulose (MC) and chemically cross-linked MC via urethane linkage (MCPU). In MC, the temperatures of the three transitions have demonstrated an increase with increasing molecular weight but no effect of molecular weight has been observed in MCPU. The result indicates that cross-linking restricts hydrophobic aggregation that has been confirmed by AFM. The fractional conversion of the gel formation in poly (urethane) dispersions was observed by Madbouly and Otaigbe (2006). Resulting data from isoconversional analysis of the resulting data showed that the effective activation energy of the process is practically constant and similar to the value determined from the temperature dependence.

Shah and Paul (2006) studied the effect of purge gas (nitrogen/air) on thermal degradation of organoclay and found that there was no difference. They concluded that it thermally drove with slight oxidative contribution. Xie, Gao, Pan, Hunter, Singh, and Vaia (2001) set 700 ºC as the upper limit for dehydroxylation of the montmorillonite, whilst Xi, Martens, He, and Frost (2005) referred to 636 ºC as an upper limit. However, a derivative thermogravimetric analysis (DTGA) curve of the parent KpF montmorillonite suggested that dehydoxylation was not fully complete until the higher temperature reaches 850 ºC (Hedley & Yuan, 2007). As thermal characteristics of some phosphonium-modified montmorillonite were discussed.

Xie, Pan, Hunter, Koene, Tan, and Vaia (2002) have separated the curves into 4 distinct regions which are : (1^{st}) evolution of free water and gasse (< 150 ºC); (2^{nd}) evolution of organic substance (≥ 150 ºC and ≤ 550 ºC); (3^{rd}) dehydroxylation of the montmorillonite (≥ 550 ºC and ≤ 700 ºC) and (4^{th}) evolution of carbonaceous residue (≥ 700 ºC and ≤ 1000 ºC). According to the researchers, the thermal behaviour of the organoclays in the 2^{nd} region is very important in terms of their function as nanofillers of polyolefins since it is in the temperature range where the interlayer begin to degrade. They did conclude that montmorillonite modified with quaternary phosphonium ions have a greater thermal stability than their quaternary ammonium-modified counterparts. Shah and Paul (2006) also observed that the mass loss of surfactants from the interlayer space of montmorillonite in the polyethylene nanocomposite was greater than that during thermo gravimetric analysis of the organoclay with polymer at onset temperature. The researchers described this to the greater ease with which degradation products are solubilised in polyethylene as compared with their evaporation from the pristine organoclay during TGA. Hedley et al. (2007) concluded that their research demonstrated the thermal properties of organoclays can vary because of differences in the nature and the arrangement of the intercalated surfactants.

The thermal degradation behaviour of polyvinyl alcohol and its nanocomposites with different amount of SiO_2 was examined with TGA by Chrissafis, Paraskevopoulos, Papageorgiou, and Bikiaris (2008). Three degradations were observed apart from one that takes place at temperatures below 150 ºC and which is due to evaporation of absorbed water which is about 3 wt % mass loss. The weight loss in the first and second stage with maximum decomposition rate temperature 280 and 310 ºC respectively, attributed to the decomposition of the polyvinyl alcohol by a dehydration reaction of the polymer chain. According to them, the weight loss corresponding to the first stage is about 35-36 % compared to the theoretical value for complete dehydration is 38.6 %. The decomposition temperature is shifted by about 5-10 ºC to higher temperature with increase of the silica content, which means that the dehydration process was hindered. This attributed to interactions taking place between the hydroxyl groups of SiO_2 proven by FTIR spectroscopy.

Peng et al. (2005) reported that for the third weight loss process, the stage was shifted at higher temperature after the addition of SiO_2 nanoparticles. Due to presence of SiO_2 nanoparticles, the thermal degradation of the nanocomposite compared to that pure polyvinyl alcohol, occurs at higher temperatures and requires more reaction activation energy and possesses higher reaction order. However, researchers found that except the decomposition temperatures the introduction of nanoparticles leads to a remarkable change in the degradation mechanism (Peng & Kong., 2007). According to Krkljes, Marinovic, Kacarevic, and Nedeljkovic (2007), a normal thermal degradation of polyvinyl alcohol and argentums nanocomposite proceeds in two degradation steps. With the inclusion of Argentums, it was seen to proceed with one step degradation. Thermal degradation of plain polypropylene is related to the endothermic effect and occurs before the mass loss starts.

Bertini, Canetti, Audisio, Costa, and Falqui (2006) studied the effect of montmorillonite on polypropylene nanocomposites in the form of fibres. They found that all weight loss temperatures for the nanocomposite fibres are higher than that of pure polypropylene fibre, which attributed to the restriction of the motion of organics chain on montmorillonite clay. It was also stated that the polypropylene/DM-MMT fibres seems to have the highest thermal stability, relative to polypropylene/Na-MMT fibres. Montmorillonite modification would also lead to further improvement of polypropylene thermal stability. A TGA analysis by Chowa and Tham (2009) in inert atmosphere showed an 87 ºC marked increase in the thermal degradation temperature in organo-treated montmorillonite. The formation of nanocomposite depends on the type of surfactant, polarity of surfactant, polymeric nature and processing condition. Different OMT and methods have influence on the morphology and thermal stability of polypropylene/clay nanocomposite (Sharma & Nayak, 2009). Except MMT modification with organic compounds the addition of 20 % PP-g-MA with C20a treated nanoclay around 90 ºC causes a further enhancement in thermal stability of polypropylene (Sharma, Nema, & Nayak, 2010).

Investigation of kinetic of degradation using Coats-Redfern models shows that simultaneous incorporation of OMMT and $CaCO_3$ nanocomposites significantly enhances the activation energy of degradation. Comparative study of the effect of different nanoparticles (such as montmorillonite and SiO_2) on the mechanical properties, permeability, and thermal degradation mechanism of HDPE was done by Chrissafis, Paraskevopoulos, Tsiaoussis, and Bikiaris (2009). It was found that HDPE, and the samples with different nanoparticles, present a relatively good thermostability since, no significant mass loss (less than 0.5%) occurred until 300 ºC. The first derivative peak presented a small increase at highest decomposition rate temperature due to the incorporation of nanoparticles. Chrissafis, Paraskevopoulos, Pavlidou and Bikiaris (2009) reported that, with an increase in nanoparticles amount, the maximum decomposition rates increases to a small extent. According to the researches, the maximum decomposition rates increased because the shielding effect of nanoparticles is more effective when the nanoparticles content is higher. Nanoparticles such as montmorillonite are used commonly to enhance the thermal stability of high density polyethylene (HDPE).

According to Min, Kim, Choi, and Lee (2006), HDPE-MMT nanocomposites degrade at higher temperature than that of neat HDPE. The temperature of 5 % weight loss is shifted up to 15 ºC by the addition of as low as 1 phr of MMT. Higher amount of MMT is unfavourable as exemplification by temperature shift only 10 ºC when the content of MMT is 2 phr. According to the researchers, this is because the nanoparticles tend to aggregate at higher concentration and the nanocomposite may shift to microcomposite. However, certain researches have suggested that the addition of clay has different effect on different thermal degradation stage of PE. An observation by Zhao, Qin, Gong, Feng, Zhang, and Yang (2005), showed that the initial stage of the degradation, in nitrogen atmosphere before 400 ºC, due to the Hofmann elimination reaction and the catalysed degradation, the polyethylene-clay nanocomposites degrade faster than pure polyethylene. At a temperature higher than 400 ºC, polyethylene-clay nanocomposites are more stable than pure polyethylene too. According to Li, Yu and Yang (2005), when the clay is exfoliated the thermal stability of polystyrene significantly increased for this reason.

Essawy, Badran, Youssef, Elfettouh, and Elhakim (2004) studied on polystyrene-montmorillonite nanocomposites prepared by in situ intercalative polymerization with influence of the surfactant type. The nanocomposites exhibited better thermal stability above 400 ºC compared to pure polystyrene. The organically modified nanocomposites showed marked improvements in both the onset and mid-point temperature of degradation (Chigwada, Wang, Jiang, & Wilkie, 2006). The amount of char was also markedly increased which indicates that the presence of the clay does play a role in the thermal degradation in an inert atmosphere. TGA data showed that the polystyrene-organically modified montmorillonite nanocomposite have significant enhanced thermal stability. The thermal stability of polystyrene nanocomposite becomes better with the increase of the organoclay amount. Ismail and Munusamy (2007) found that the incorporation of OMMT and MAH does not influence the degradation mechanism of polyvinyl chloride but it alters the degree of degradation. When an organomodification agent used, it was found that octadecylamine accelerates polyvinyl chloride degradation.

Peprnicek, Duchet, Kovarova, Malac, Gerard, and Simonik (2006) showed that TGA revealed that the thermal stability strongly depends on PVC-nanoclay interactions. In other words, organophilic treatment improves the thermal stability of PVC-nanoclay composite due to better interactions between PVC matrix and clay. ABS-MMT nanocomposites prepared by direct intercalation through one step emulsion polymerization. The onset temperature of decomposition shifted to the higher temperature region as much as 40–50 ºC when the MMT content reached 33.3 wt %, though the direct intercalation was not accompanied by delamination of the clay layers. ABS-clay nanocomposites was synthesized by using two clays (sodium montmorillonite and laponite). Both colloidal stability and mechanical properties of the nanocomposites depended on aspect ratios of clays (Choi et al., 2005). It was found that the onset temperatures of thermal decomposition of nanocomposites shift towards a higher temperature compared with neat ABS. The neat ABS showed 20 % weight loss at 420 ºC, but ABS clay nanocomposites decomposed at 13 ºC higher temperature. According to Cai, Huang, Xia, Wei, Tong, Wei, and Gao (2010), the type of organic modifier would affect thermal stability of ABS.

2.3 Differential Scanning Calorimetry Analysis of polymer with minerals

By taking into account the polymorphism of isotactic poly (propylene), the researchers suggest that the curve from T_g to 60 ºC reflects crystallization of mesomorphic isotactic poly (propylene) by homogeneous nucleation, whereas the curve from 60 ºC to T_m represents the monoclinic α-form by heterogeneous nucleation. In the discussion of irregularly shaped DSC exotherms that accompany isothermal and nonisothermal crystallization of poly (3-hydroxybutyrate) by Dilorenzo, Sajkiewicz, Lapietra, and Gradys (2006), they explained that the crystallization of the extremely pure polymer occurs via the growth of a very few nuclei so that the irregularities in the heat flow reflect individual acts of nucleation.

Hargis and Grady (2006) have done an investigation on the effect of non-ideal heat transfer on crystallization of low and high density polyethylene as measured by DSC. As a result, for thicker samples measured at lower temperatures, slower crystallization rates have been identified. However the difference due to sample thickness has disappeared at higher temperatures, suggesting that finite heat transfer rates are responsible for the effect. Lorenzo, Arnal, Albuerne and Muller (2007) provided a practical guide to fitting DSC data on isothermal crystallization of polymers to the Avrami equation. Cai, Li, Han, Zhuang, and Zhang (2006) have tried to combine DSC and polarized light microscopy to follow crystallization and crystal morphology of syndiotactic 1, 2-polybutadiene. The Hoffman-Lauritzen parameters have been estimated through isoconversional analysis of DSC data and found to be in the agreement with the parameters derived from the microscopy measurement. Botines and Puiggali (2006), have studied crystallization of poly (glycolic acid-alt-6-amino-hexanoic acid). In their study of nonisothermal crystallization of short carbon fibre-poly (trimethylene terephthalate) composites.

Run, Song, Yao, and Wang (2007) have found that the addition of the fibre promotes nucleation. It was reported that the effect is to easily seen by itself in the nucleation parameter of the Hoffman-Lauritzen theory. Effect of nanosize fully vulcanized acrylic rubber powders on crystallization of poly (butylene terephthalate) has been explored by Huang (2007), who analyzed the resulting DSC data in terms of the Hoffman-Lauritzen theory. The result revealed that the rubber nanoparticles hinder crystallization at smaller loads but may act as heterogeneous nucleation centres as the load increases. High density polyethylene (HDPE)-carbon nanotube nanocomposite by in situ polymerization of ethylene on carbon nanotubes (CNT) treated with a metallocene catalyst was produced by Trujillo, Arnal, Mueller, Laredo, Bredeau, Bonduel, and Dubios (2007). DSC studies have shown that CNT make more efficient nucleating agent than HDPE. Following that, Sargsyan, Torloyan, Davtyan, and Schick (2007) applied DSC to study the relaxation behaviour in a model PMMA-SiO_2 nanocomposite. Measurements of heat capacity demonstrate that the nanocomposite contains an immobilised polymer fraction which can simulate the behaviour of RAF. As a result, the rigid crystals must melt before the RAF can relax.

Rastogi, Lippits, Hohne, Mezari, and Magusin (2007) performed DSC analysis of the melting behaviour of ultrahigh molecular weight polyethylene and indicated that at low heating rates, the crystals melt by consecutive detachment of chain stems whereas several chain stems involved at high heating rates by melting of clusters. Evolution of the melting enthalpy on annealing at different temperatures suggest that the existence of three different melting process characterized by different activation energies that reflect different degrees of cooperation. Sbirrazzuoli, Mititelu-Mija, Vincent, and Alzina (2006) has managed to evaluate the activation energies for the primary amine reaction, etherification and homopolymerization as 55-60, 104 and 170 kJ mol^{-1} respectively by analyzing the curing kinetics of stoichiometric and nonstoichiometric mixtures, diglycidyl ether of bisphenol-A and 1, 3-phenylene diamine. DMA measurement by Miyagawa, Rich, and Drzal (2006) on epoxy nanocomposites reinforced by fluorinated single wall carbon nanotubes (FSWCNT) have shown that an addition of FSWCNT will actually decrease the glass transition temperature of the cured epoxy. After adjusting the amount of the anhydride curing agent for stoichiometry, they have found that the reinforced materials have markedly larger storage modulus compared with the anhydride-cured neat epoxy.

DSC has been used by Liu, Xie, Yu, Chen, and Li (2009) to monitor the evolution of glass transition temperature through out the isothermal cure of endodicyclopentadiene with Grubbs catalyst. The glass transition temperature versus conversion data fell on a single curve independent of cure temperature, implying that the reaction proceeds in a sequential fashion. Ramis, Morancho, Cadento, Salla, Fernandez, and Franco, (2007) have demonstrated that oxygen has an inhibiting effect on the photopolymerization of a mixture of two dimethacrylates. Accoding to researchers, by increasing the intensity of UV radiation, the effect could be overcome.

The utility of the thermal analysis methods as applied to thermosets formed by free radical photo curing was illustrated by Chartoff (2006). The methods displayed that they are capable of revealing that the polymers contain more than one phase even if only one monomer is involved; an unusually broad glassy samples trap free radicals that continue to react slowly; the degree of conversion attained in many UV cured system do not rise above 60-80%; incompletely cured glassy samples trap free radicals that continue to react slowly; partially heating of a cured polymer above its glass transition temperature. Cai, Sun, Wang, and Zhou (2007) studied the process of curing of a novel epoxy containing a tetramethylbiphenyl and aromatic ester type mesogenic group with diaminodiphenylsulfone. Isoconversional kinetic analysis of the DSC data has revealed a change in curing mechanism associated with formation of liquid crystalline structure detected by hot storage polarized light microscopy.The curing kinetics has been monitored as disappearance of the 915 cm^{-1} epoxy bending absorption and revealed a complex mechanism through isoconversional analysis (Cervellera, Ramis, Salla, Mantecom, & Serra, 2007).

He and Yan (2007) have studied on curing kinetics of polymeric diphenylmethane with different wood species under the oven dry, explaining that the dominant mechanism of curing is the reaction between water and isocyanate compound. Hernandez, Dupuy, Duchet, and Sautereau (2007) have also studied the curing kinetics but it was in a ternary system epoxy-PMMA and stated that there were delays in the reaction until the phase separation occurs. However, the addition of clay accelerates the curing reaction most likely due to a catalytic effect of metal ions in the clay. According to Chrissafis and Bikiaris (2011), there was higher onset temperature for nanocomposites that incorporated with 1 % and 3 % clay than polyethylene. However, when the loading of clay reaches 5 %, the onset temperature is decreased, suggesting the promoter effect has an influence on thermal stability. The clay seemed to have two opponent effects in the thermal stability of polymer-clay nanocomposites. A study on ultra high molecular weight polyethylene-organaoclay hybrid nanocomposite (UHMWPE) by Lee, Oh, Ha, Jeong and Kim (2009) showed that thermal resistance is enhanced in the presence of nanoclay due to the thermal insulation effect of clay.

A study on the thermal stability of polyethylene-MMT nanocomposite was conducted by Stoeffler, Lafleur, and Denault (2008) and it was observed that in argon atmosphere, no significant variations in ttemperature at 10 wt % and 50 wt % degradation were observed between the various formulations. The effect of different nanoparticles has also no effect of thermal degradation of LDPE. Moreover, Garcia, Hoyos, Guzman, and Tiemblo (2009) studied the thermal degradation under nitrogen and air flow of LDPE and three 5 wt % nanocomposite based on this polymer matrix. According to Costa, Wagenknecht, and Heinrich (2007), addition of even a small amount of LDH improves the thermal stability and onset decomposition temperature in comparison with the unfilled LDPE.

A report by Giannakas, Xidas, Triantafyllidis, Katsoulidis, and Ladavos (2009) showed that the thermal stability of the low density polyethylene was not affected with the addition of 10 wt % organosilicate. This was concluded because both the neat polymer and the other composites begin to reduce in weight at similar temperatures. In general, for Ethylene vinyl acetate (EVA), the thermal degradation proceeds in two steps. The first step is the loss of acetic acid followed by the degradation of the remaining partially unsaturated polyethylene polymer (Costache, Jiang, & Wilkie, 2005). The first step is reported to be accelerated by the presence of clay. It was also shown that the clay does affect the degradation pathway and the presence of hydroxyl groups on the edge of the clay is caused by the accelerated initial step. Organically modified clay could accelerate the degradation of EVA since it can affect both the first and second decomposition step of EVA (Szep, Szabo, Toth, Anna, & Maros, 2006). Elimination of the acetyl acid is promoted by each of the organophilised montmorilloinite resulting in weight-losses starting at lower temperature than without. According to the researcher, modified montmorillonite intercalated and shifts the beginning of the decomposition to higher temperature but the non modified montmorillonite seemed to catalyse the main degradation step.

Zhang, Ding, Zhang, and Qu (2007) studied the thermal degradation behaviours of pure EVA and various EVA-ZnAl-LDH samples prepared by melt intercalation and solution intercalation respectively. The report showed that all nanocomposites samples respond with an increased thermal stabilities compared with pure EVA, the thermal degradation temperatures increase with increasing the LDH loadings. A report by Bourbigot, Gilman, and Wilkie (2004), suggested that the thermal stability of polystyrene increases with the presence of the clay under both pyrolytic and thermo-oxidative conditions. The researchers showed that the clay acted as a char promoter. A char prometer slows down the degradation process and provides a transient protective barrier to the nanocomposite.

2.4 FTIR analysis of polymer with clay mineral

According to Vaccari (1999), clay mineral can act as catalyst to accelerate the hydrolysis and gelation process because of the Bronstead and Lewis acid sites on the external surface. Wu, Qi, Wang, and Xin (2010) observed the FTIR spectra of untreated and treated montmorillonite and showed that the comparison with spectrum of untreated montmorillonite. The absorption peaks at 3625 and 3440 cm^{-1}, showed the stretching mode of O-H, and the absorption peaks at 916 and 847 cm^{-1}, showed the –OH bending vibration of hydroxide of the nanocomposite. Ma, Tong, Xu, and Fang (2008) conducted a research on flame retardant of ABS-MMT. FTIR spectra of the residue showed that the absorbance at 1043 cm^{-1} and 1625 cm^{-1} are due to vibration of Si-O and aromatic structure formed because the barrier effect of the mineral clay, respectively.

Tang, Zou, Xiong, Tang, and Huali (2005) reported that due to the stretching vibrations of CH and CH_2 groups, the absorption band for pure polyvinyl alcohol compound with all organic compounds is seen at 2391 cm^{-1}. Other than that from the IR analysis, it was concluded that with the increase in nano-SiO_2 amount, there was an increase in the intermolecular hydrogen bonds between nano-SiO_2 and PVA. Fourier transform infrared (FTIR) spectra of the thermoplastic starch showed a downward shift in the hydroxyl stretch indicative of a disruption in H-bonding between starch chains during extrusion processing and with the inclusion of polyvinyl alcohol, the an upward shift in the hydroxyl stretch was observed. With the addition of Na-MMT the H-bonding between the PVOH and starch was disrupted (Dean, Do, Petinakis, & Yu, 2008).

2.5 Mechanical properties analysis of polymer with clay mineral

Looking into mechanical properties, Majdzadeh and Nazari (2010) studied the effect of PVOH content on the clay nanocomposites and reported that the highest value of modulus and elongation was achieved when 5 wt % PVOH is used. The lower or higher levels of PVOH do not result in proper tensile properties. Dean et al. (2008) found similar behaviours when they compared the effects of 0 %, 2 %, 5 % and 7 % by weight of PVOH on tensile properties in extruded starch-PVOH-clay nanocomposites. According to the researchers, adding in higher content of polyvinyl alcohol into the composite does not enhance the overall mechanical properties. Higher content of polyvinyl alcohol indirectly increases the interactions between polyvinyl alcohol-starch compound which would battle with the interaction between all three polyvinyl alcohols, starch and the clay surface. Although a good dispersion of clay platelets is important in improving mechanical properties in nanocomposites, the interfacial interactions of filler and matrix starch-PVOH plays an important role.

According to Selvakumara, Palanikumar, and Palanivelu (2010), both the tensile strength and modulus of polypropylene-MMT nanocomposites increase from 0 wt % to 5 wt % clay concentration. Dean et al. (2008) studied the key interaction in biodegradable thermoplastic starch-polyvinyl alcohol-montmorillonite micro- and nanocomposites. The researcher showed that, there was a slight plasticising effect as polyvinyl alcohol is added from 2 wt % to 7 wt % where it indirectly gives higher percentage elongation at break. On the other hand, in the nanocomposites containing no PVOH, increasing the Na-MMT content was shown to significantly increase the modulus. Increasing the Na-MMT content was also shown to increase the tensile strength up to 67 % and a small drop in elongation at break.

According to Schlemmer, Angelica, Maria, and Sales (2010), the introduction of low content (≤ 5 wt %) of MMT improves both the stiffness and thermal stability of a material. (Cyras et al., 2008) observed an important increase of five and sixfold in the modulus when 3 wt % and 5 wt % of MMT compared to the starch in the starch-clay system. Huang, Yu, and Ma (2006) observed that the Young's modulus increases with increasing MMT amount, however the increment was more important when up to 5 wt % of clay was added to the starch.

CHAPTER 3

METHODOLOGY

3.1 Materials

Completely hydrolysed polyvinyl alcohol Denka POVAL grade K-17C with viscosity of 24-30 mPa s, hydroysis 98.7 ~ 99.7 mol% and ash less than 0.7% manufactured by Denki Kagaku Kougyo Kabushiki Kaisya (DENKA) was used in this study. Native corn starch was purchased from Thye Huat Chan Sdn Bhd. Nano-size montmorillonite clay was purchased from Timlewis (M) Sdn. Bhd.

3.2 Formulation

The amount of MMT was varied respectively starting from 0.1 g, 0.3 g, 0.5 g, and 0.7 g to 0.9 g. The amount of PVOH was also varied respectively from 20 wt %, 30 wt %, 40 wt %, and 50 wt % to 100 wt %. Table 3.1 below shows the composition of PVOH - corn starch added with MMT which was involved in this research

Table 3.1: Composition of PVOH-corn starch added with MMT

Sample	PVOH: CRS (wt %)	PVOH (g)	CRS (g)	MMT (g)
PCM-28-1	20:80	2	8	0.1
PCM-37-1	30:70	3	7	0.1
PCM-46-1	40:60	4	6	0.1
PCM-55-1	50:50	5	5	0.1
PM-1	100:0	10	0	0.1
CM-1	0:100	0	10	0.1
PCM-55-3	50:50	5	5	0.3
PM-3	100:0	10	0	0.3
PCM-55-5	50:50	5	5	0.5
PM-5	100:0	10	0	0.5
PCM-55-7	50:50	5	5	0.7
PM-7	100:0	10	0	0.7
PCM-55-9	50:50	5	5	0.9
PM-9	100:0	10	0	0.9

3.3 Sample preparation

Solution cast samples of PVOH-CRS-MMT are prepared as shown on the table above. Samples PCM-28, PCM-37, PCM-46 and PCM-55 were prepared by dissolving both PVOH and MMT in distilled water and heated in water bath at about 97± 2 ºC for 30 minutes until all PVOH particles dissolved. In a study of PVOH particles (Kuraray Specialities, 2003), fully hydrolysed PVOH requires a minimum temperature of 90 ºC in order to dissolve in water. The amount of MMT was increased from 0.1g to 0.9g. As the PVOH dissolves completely in distilled water, the corn starch (CRS) is added. The mixture of PVOH-CRS-MMT was then heated once again in the water bath at 97± 2 ºC for 30 minutes.

On the other hand, for samples PM and CM, neat PVOH and CRS were heated together with MMT respectively. The samples were heated in water bath for about 1 hour. A motor driven stirrer with appropriate rpm (800 rpm) was used to stir the mixtures firmly. The mixtures were cast in the form of film onto Petri dishes and dried in a vacuum oven at about 65 ºC to achieve a constant weight. At least 10 samples were prepared for each test. The samples were then immediately sealed in a polyethylene bags and stored under room temperature 25 ºC at 65% relative humidity for conditioning purpose.

3.4 Testing

3.4.1 Mechanical properties (Tensile test)

Tensile strength and percentage elongation at break was tested according to ASTM D882 standard. The mixtures were cast in the form of standard rectangular-shaped. The specimens' width and thickness are measured. The specimen is placed in the grips of the Instron 5848 Microtester taking care to align the long axis of specimen and the grips with an imaginary line joining the points of attachment of the grips to the machine.

3.4.2 Thermal properties (DSC)

Differential Scanning Calorimerty (DSC) analysis was conducted using Perkin Elmer DSC7. The DSC thermograms were used to obtain the onset, endpoint melting temperatures and the enthalpy of melting for the samples.

3.4.3 Physical properties/ Morphologies (SEM)

The surface morphology of the surface of the films, after incorporated with MMT was investigated using Hitachi Scanning Electronic Microscopy of BS 340 TESLA.

3.4.4 Interaction of bonding

Fourier Transform Infrared (FTIR) analysis was conducted using the Perkin Elmer Spectrum One. The Potassium Bromide (KBr) pellet method was used to observe the IR spectrum. The PVOH – corn starch – MMT films were grounded into an agate mortar together with KBr into powder form to reduce the particle size to less than 5 mm in diameter and until there were no crystallites seen. The powder was then filled into a press where a thin and transparent pellet is formed. The pellets were then placed into the sample holder for scanning. The scanning was done in a region of 4000 – 400 cm^{-1}.

3.5 Calculation

The crystallinity of the samples are calculated based upon 161 J/g for the 100 % crystalline PVOH as a reference material (Blaine, 1990). Equation 3.1 below shows the way to calculate the crystallinity of a blend and. A sample calculation for the crystallinity (%) is also shown below:

$$Crystallinity = \frac{\Delta H_m}{100\ \%\ Crystallinity\ of\ PVOH} \times 100\ \% \qquad (3.1)$$

Where

ΔH_m = Enthalpy of melting, J/g

100 % Crystallinity of PVOH = 161 J/g

Thus, when the Enthalpy of melting (ΔH_m) = 55.33 J/g

$$Crystallinity = \frac{55.33}{161} \times 100\ \%$$
$$= 34.37\ \%$$

CHAPTER 4

RESULTS AND DISCUSSION

4.1 Mechanical properties

4.1.1 Interaction of neat PVOH with various amount of MMT

Tensile test for this project showed that all samples had an initial period of elastic deformation followed by a nearly monotonically increasing stress during plastic deformation, until failure. Figure 4.1 shows the tensile strength of nanocomposite with neat PVOH and various amount of MMT. 100 % of PVOH was incorporated with various amount of MMT such as 0.1 g, 0.3 g, 0.5 g, 0.7 g and 0.9 g. From the graph, it can be seen that, as the amount of MMT incorporated together with PVOH increases from 0.1 to 0.5 g, the tensile strength increases. For the sample with higher loading above 0.5 g of MMT, the tensile strength begins to decrease. The highest tensile strength of 16.0 MPa was achieved when 0.5 g of MMT was incorporated with the neat PVOH. This is because, at a low loading of MMT content (0.1-0.5 g), as the amount of MMT increases, the nano-sized MMT tend to attach efficiently onto the PVOH structure. However, excess amount of MMT (above 0.5 g) was believed to have a phase separation and poor particle distribution which eventually weakens the tensile strength.

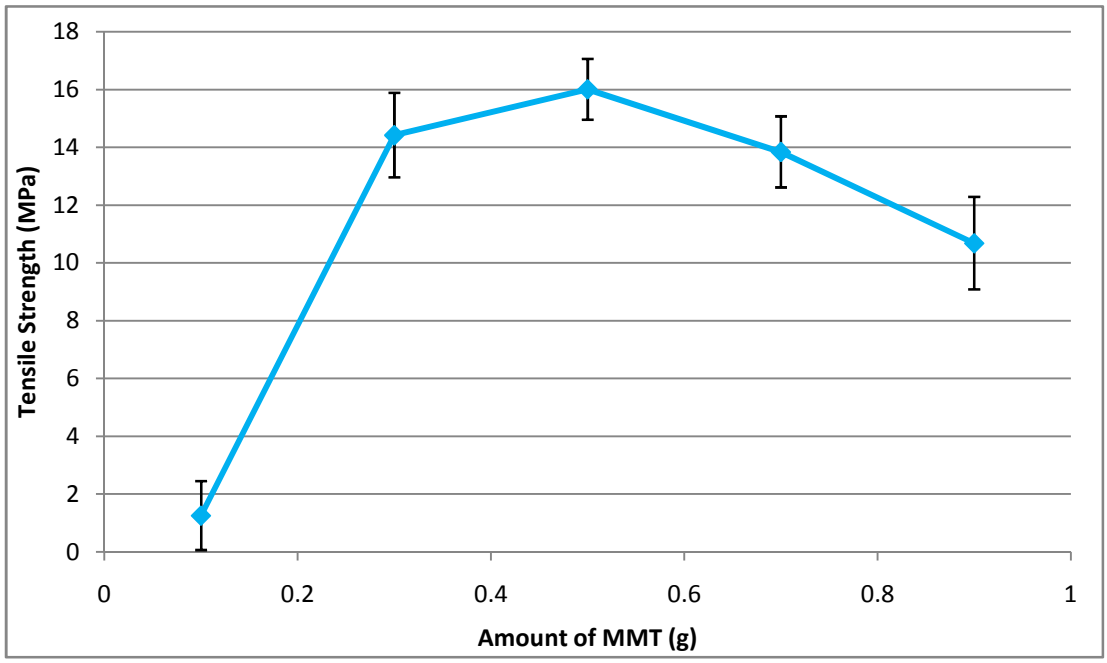

Figure 4.1: Tensile strength of neat PVOH – MMT blends

Similarly, from Figure 4.2, the percentage elongation at break increases as the amount of MMT increases from 0.1 g to 0.5 g and begins to decrease for further incorporation of MMT content. The highest percentage elongation at break of 82.7 % was achieved when 100 % PVOH is incorporated with 0.5 g of MMT. Samples with 100 % PVOH showed higher percentage elongation compared to samples with 50 % of PVOH (Figure 4.5) because the plasticising deformation had increase with the increment of PVOH amount into the blend. Similar results were obtained by Dean et al. (2008) when the effect of PVOH on PVOH-Starch-Clay nanocomposites was compared.

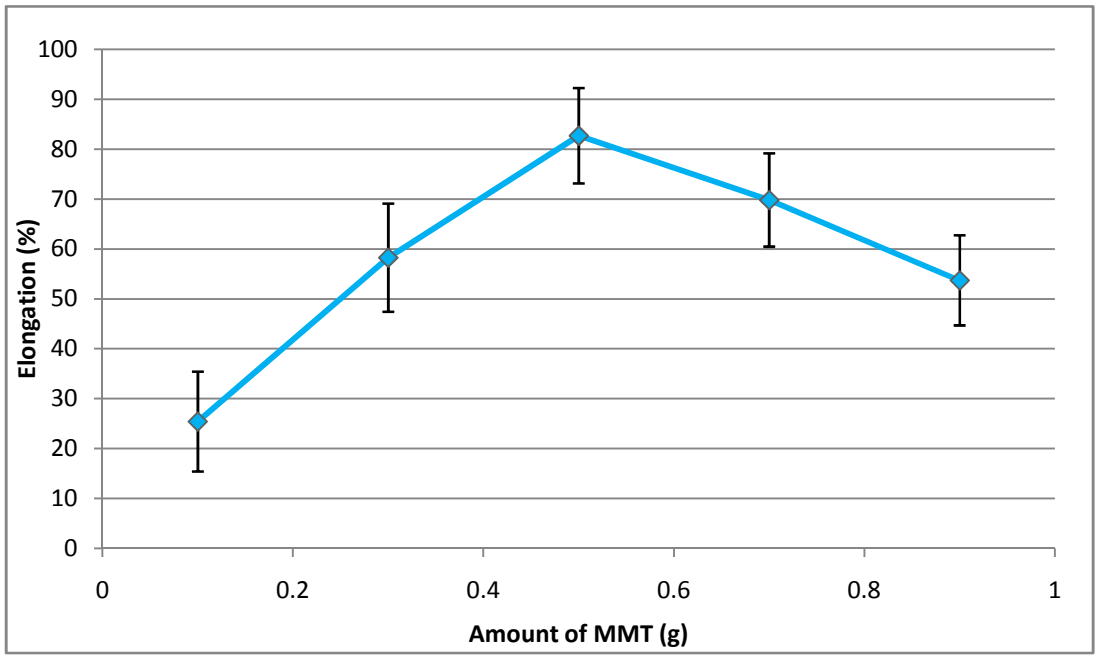

Figure 4.2: Percentage elongation at break of neat PVOH – MMT blends

The modulus increases with the increasing amount of MMT, as it is for most of the conventional filled polymer system. Figure 4.3 shows the modulus of the neat PVOH incorporated with MMT. For the neat PVOH sample, the highest modulus of 86.5 MPa was achieved when it was incorporated with 0.9 g of MMT. The modulus value increases with increasing amount of MMT due the strong interaction between matrix and silicate layers via formation of hydrogen bonds, due to the strong hydrophilicity of the clay edges (Sengwa, 2009). This is probably also similar to a report from Ryan, Cadek, Nicolosi Blond, Ruether, and Armstrong (2007) where similar increase of modulus of PVOH with the addition of carbon nanocomposites was reported. It was suggested that in semi-crystalline polymer like PVOH and nanocomposite systems, the formation of nanocomposite induced crystalline polymer domains were the dominant reinforcement mechanism and there were no stress transfer for the nanocomposites.

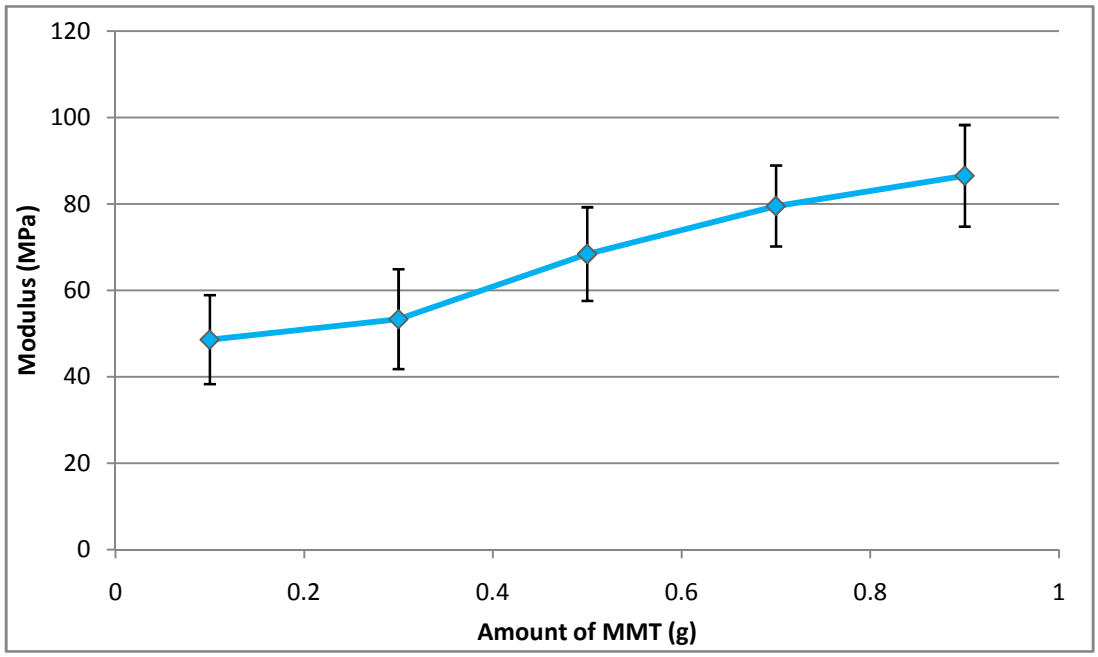

Figure 4.3: Modulus of neat PVOH – MMT blends

4.1.2 Interaction of 50 % PVOH with various amount of MMT

Figure 4.4 shows the tensile strength of nanocomposite with 50 % PVOH incorporated with various amount of MMT. 50% of PVOH were blended with various amount of MMT such as 0.1 g, 0.3 g, 0.5 g, 0.7 g and 0.9 g. From the graph, the tensile strength increases with the increasing amount of MMT. There was a slight decrease in tensile strength for the sample with 0.7 of MMT. However, it can be clearly seen that the highest tensile strength of 26.4 MPa was achieved when 50 % of PVOH was incorporated with 50 % of corn starch and 0.9 g of MMT.

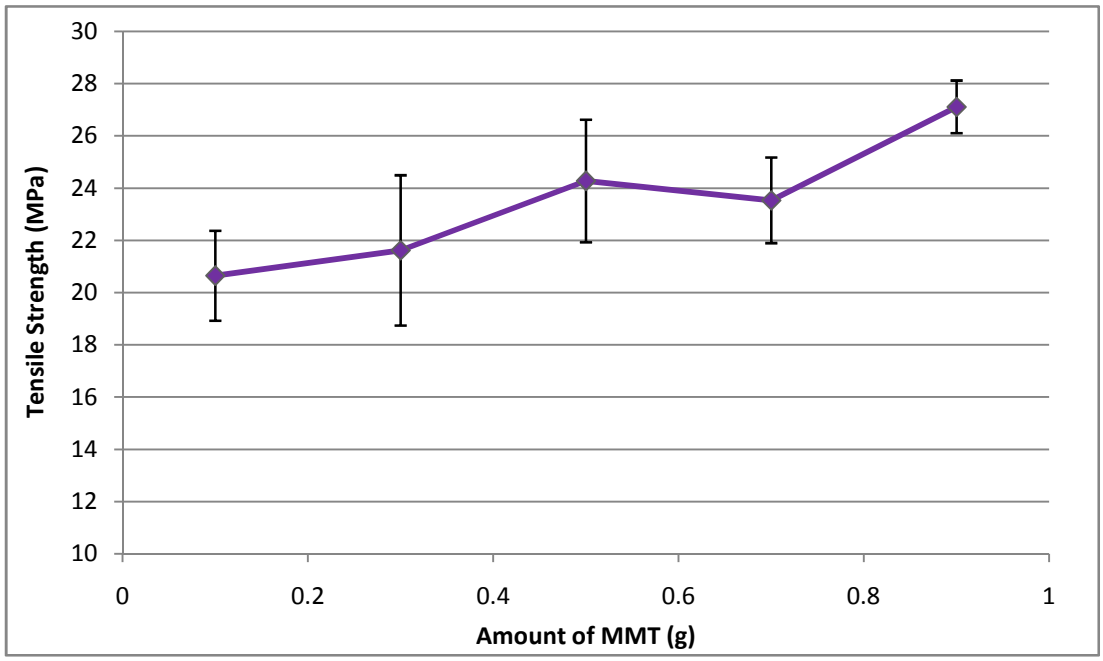

Figure 4.4: Tensile strength of 50 % PVOH – MMT blends

In this case, SEM images suggested that, when the amount of MMT incorporated with 50 % of PVOH increased from 0.1 g to 0.9 g, agglomeration between all three different particles in decreases. In other words, the nanocomposite formed was mostly exfoliated hybrids. This result might be different compared to the samples with neat PVOH because for the samples with 50 % of PVOH, there are another 50 % of corn starch which possesses extensively strong interaction with the PVOH matrix.

This was agreeable as a report from Sin, Rahman, Rahmat, Sun, and Samad (2010) showed that the Starch-PVOH blend have experimental enthalpy of melting higher than the theoretical values. Increasing the loading of MMT into the PVOH-Starch blend promotes the disaggregation as well as the dispersion of MMT in the Starch-PVOH matrix and played the role of a reinforcing agent.

As shown in Figure 4.5, the percentage elongation at break showed similar trend as it was for the tensile strength. The percentage elongation at break increases with the increasing amount of MMT content. Incorporation of MMT increases the interaction of the nanocomposite hence presenting both higher tensile strength and percentage elongation where the MMT improves the strong existing Starch-PVOH matrix. For the samples with 50 % of PVOH, the highest percentage elongation at break of 12.3 % was achieved when they were incorporated with 0.9 g of MMT.

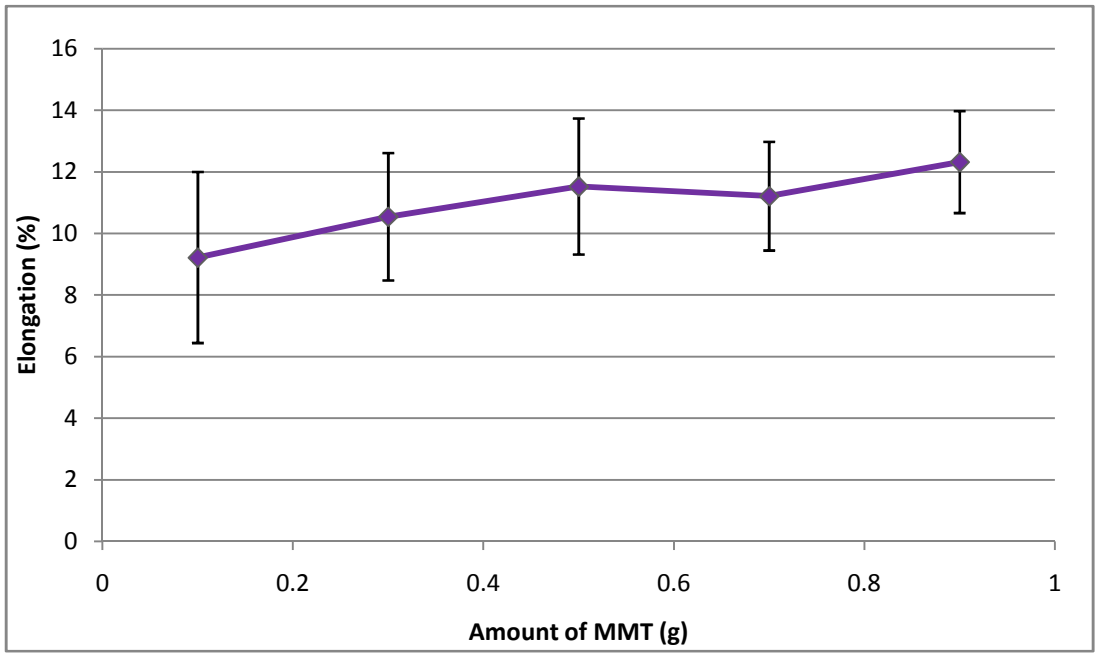

Figure 4.5: Percentage elongation at break of 50 % PVOH – MMT blends

Figure 4.6 shows the modulus obtained when 50 % of PVOH was incorporated with various amount of MMT. From the graph, when the amount of MMT increases from 0.1, 0.3, 0.5, 0.7 to 0.9 g, the modulus increases orderly. The highest modulus value of 742.3 MPa was achieved when 50 % of PVOH was incorporated with 50 % of corn starch and 0.9 g of MMT. The modulus value increases with increasing amount of MMT due the strong interaction between matrix and silicate layers via formation of hydrogen bonds, due to the strong hydrophilicity of the clay edges (Sengwa, 2009). This is also probably similar to case explained above where in semi-crystalline polymer like PVOH and nanocomposite systems, the formation of nanocomposite induced crystalline polymer domains were the dominant reinforcement mechanism and there were no stress transfer for the nanocomposites.

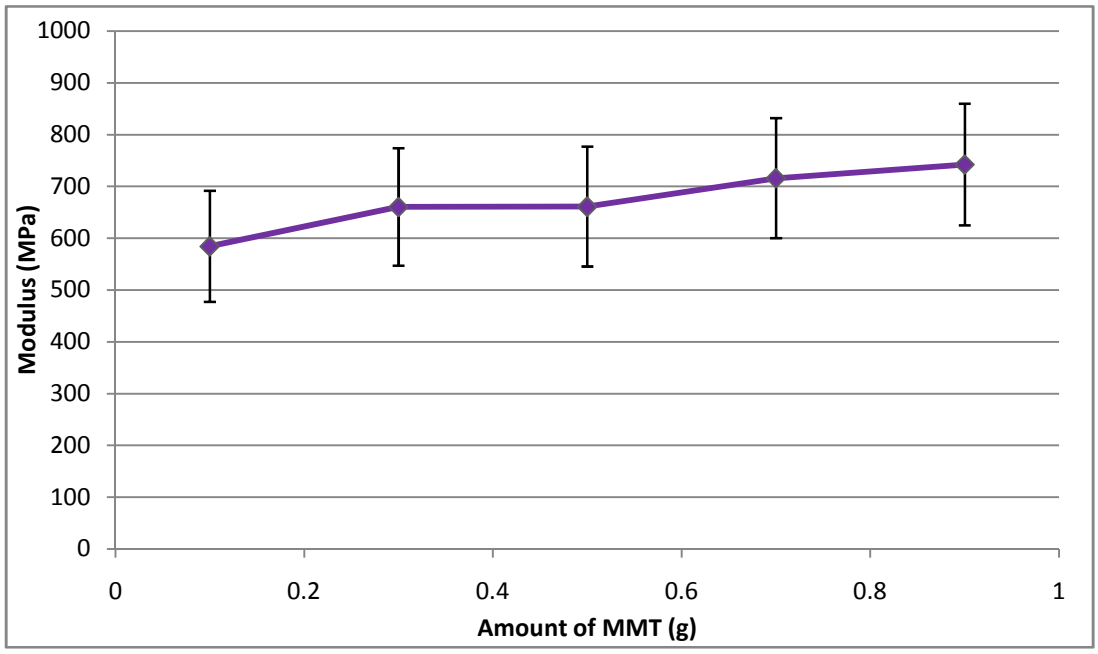

Figure 4.6: Modulus of 50 % PVOH – MMT blends

4.1.3 Interaction of 0.1 g of MMT with various amount of PVOH.

Figure 4.7 shows the tensile strength of nanocomposite with 0.1 g of MMT and various amount of PVOH such as 20 %, 30 %, 40 %, 50 % and 100 %. From the graph, it can be seen that, the tensile strength basically increases when the amount of PVOH increases. When 30 % of PVOH was incorporated with 0.1 g the tensile strength slowly increases from 2.5 MPa to 13.4 MPa. Further addition of PVOH to 40 and 50 % increased the tensile strength to 19.0 MPa and 20.6 MPa respectively. The highest tensile strength achieved was for the sample with 50 % of PVOH as further addition of PVOH to 100 % showed a drastic decrease of tensile strength to 1.3 MPa. The sample with 50 % of PVOH had the highest tensile strength compared to the other variation of PVOH because when the amount of PVOH increase, the amount of corn starch indirectly decreases. Lower percentage of starch decreases the brittleness effect that will actually increase the tensile strength. Similarly, Siddaramaiah and Somashekar (2003) insisted that tensile strength increases slightly only when 10 wt % of starch was added to PVOH.

Dean et al. (2008) found similar effect when they compared the effect of 0 %, 2 %, 5 % and 7 % by weight of PVOH on tensile strength properties in extruded PVOH-Starch-Clay nanocomposites. Besides, quite similar result was also obtained by Majdzadeh and Nazari (2010) when the influence of PVOH content on starch-clay nanocomposite has been investigated. These results show that only certain amount of PVOH improves tensile properties of PVOH – Starch – MMT blends. Further addition of PVOH more than 50 % would obviously inhibit the tensile strength of the blends because increase in the amount of PVOH leads to an increase in PVOH – starch interactions that might compete with interaction between all three PVOH, starch and MMT compounds.

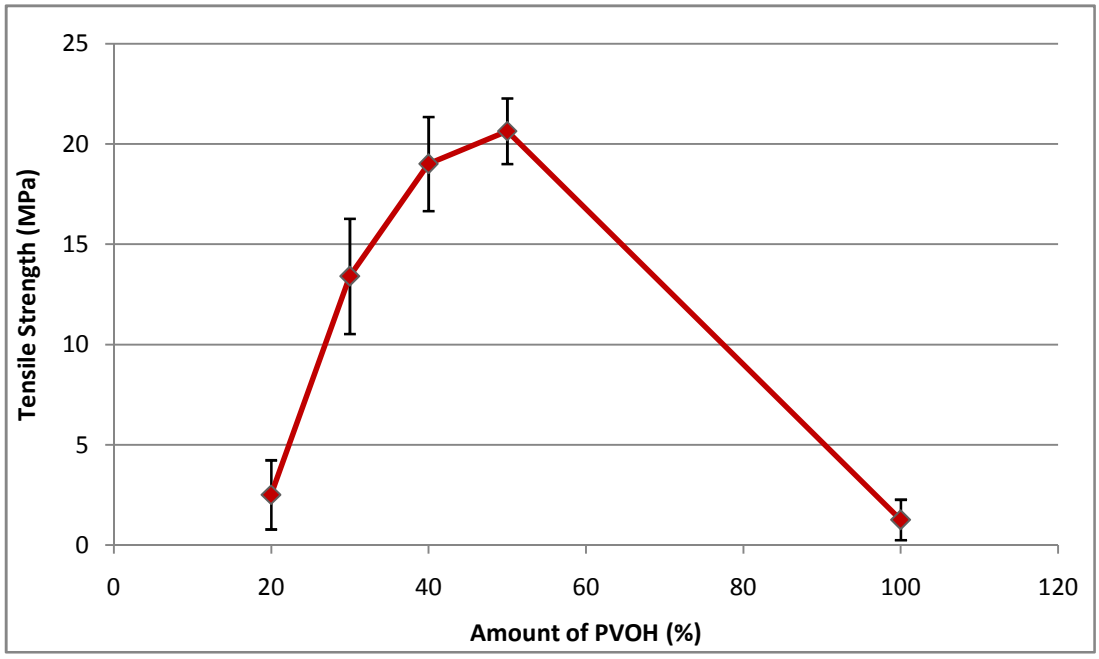

Figure 4.7: Tensile strength of 0.1 g MMT – PVOH blends

For the samples with 0.1 g of MMT, the highest percentage elongation at break of 25.4% was achieved when it was incorporated with 100 % of PVOH. From Figure 4.8, the percentage elongation at break increases proportionally with increasing amount of PVOH because the plasticising nature of PVOH was increasingly dominating the blends.

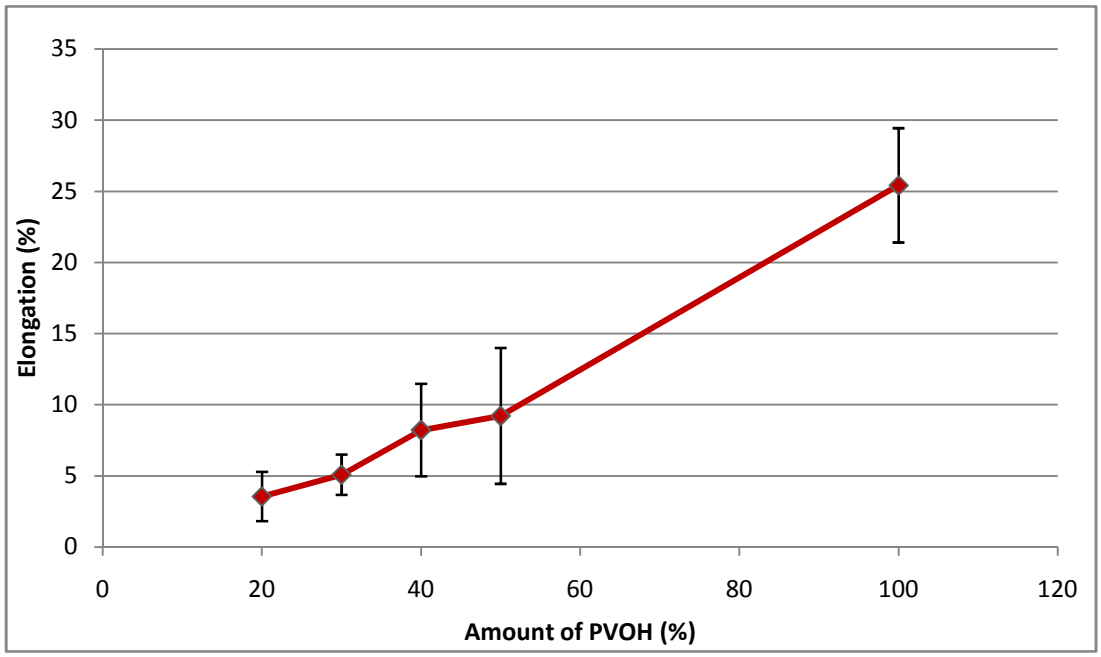

Figure 4.8: Percentage elongation at break of 0.1 g MMT – PVOH blends

According to Figure 4.9, the modulus obtained was in quite similar trend with the tensile strength. For 0.1 g of MMT, the highest modulus of 1,259 MPa was achieved when it was incorporated with 50 % of PVOH. It was even the highest modulus value obtained compared to other blending in this study. The dependence of modulus on MMT was seen to be very strong at lower incorporation of PVOH (20-50 %) into the nanocomposite. In this case, with the amount of MMT fixed at 0.1 g, the increase in PVOH content causes PVOH to become the dominant in the system hence reduces the crystallinity effect of the nanocomposite systems to more semi-crystalline structure.

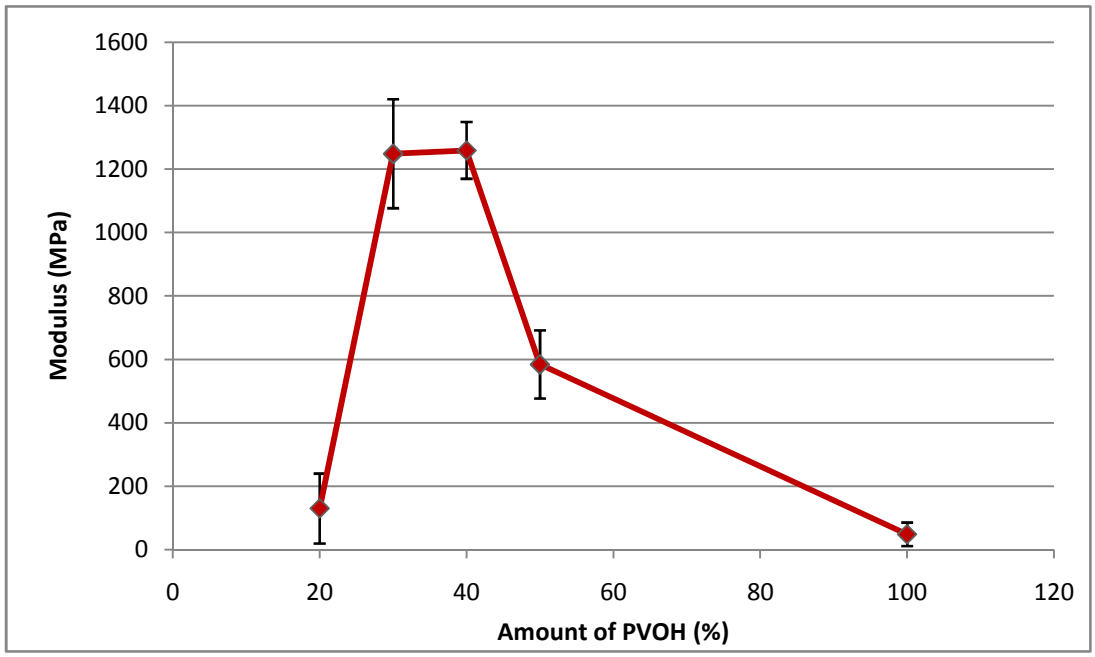

Figure 4.9: Modulus of 0.1 g MMT – PVOH blends

4.2 Thermal properties (DSC)

4.2.1 Interaction of neat PVOH with various amount of MMT

The enthalpy of melting (ΔH_m) data was extracted from the DSC thermograms. These values were used to plot graphs as shown in figure 4.10, 4.11 and 4.12 respectively. All these samples had quite narrow melting ranges with endothermic peaks throughout the heating process. Figure 4.10 shows the enthalpy of melting for the neat PVOH – MMT blends. Since CM - 1 (sample with 100% corn starch and 0.1 g of MMT) did not exhibit a melting stage, the sample was assumed not to have any influence or impact on enthalpy of melting and the intramolecular bonds between both PVOH and starch molecules. This also indicated that, sample with neat corn starch was actually in amorphous phase.

From Figure 4.10, the enthalpy of melting increases with increasing amount of MMT from 0.1 g to 0.5 g with values from 55.33 J/g to 59.56 J/g respectively. However the enthalpy of melting then was seen to decrease for further addition of MMT until it reaches as low as 53.94 J/g. The highest enthalpy was achieved with the value of 59.56 J/g for the sample containing 100 % PVOH and 0.5 g of MMT. The enthalpy of melting increases due to the presence of intermolecular interactions between the blended components. Increase in enthalpy of melting indicates that more energy was needed to break the bonding and releasing the polymer chains from its rigid crystal structure to reach melting point. Further addition of MMT (above 0.5 g) decreases the enthalpy of melting indicating that less energy was needed to break the weak bonding of the MMT-PVOH components to reach its melting point.

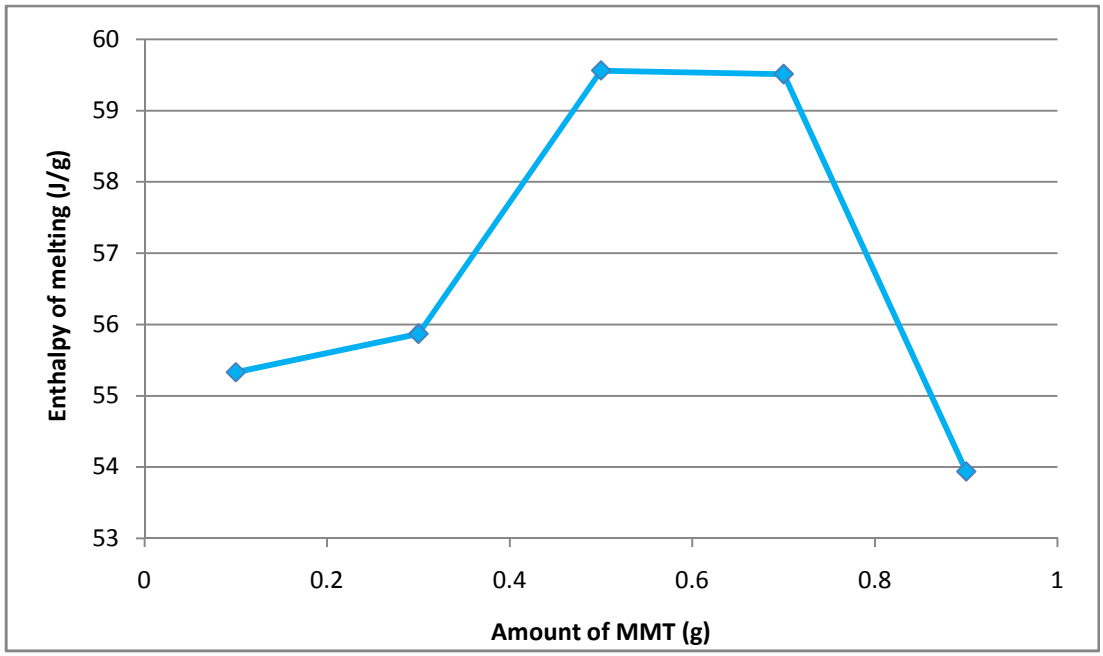

Figure 4.10: Enthalpy of melting of neat PVOH – MMT blends

Since the compositions of the compounds are varied, not all the samples in this study showed same degree of crystallinity. As showed in methodology (Chapter 3), the crystallinity of the samples are calculated based upon 161 J/g for the 100 % crystalline PVOH as a reference material (Blaine, 1990). The enthalpies of melting are divided with 161 J/g in order to obtain the crystallinity (%). Table 4.1 shows the nanocomposite crystallinity. From the table, it can be seen that, as the amount of MMT increases, the crystallinity (%) increases. However, further addition of MMT (above 0.5 g) causes decrease in the crystallinity This result was obtained because the inorganic layers of MMT below 0.5 g might have promoted a new crystalline phase, characterized by higher melting temperature and different crystal structure. The new crystal phase seems to increase the thermal properties. Similar results were reported by Strawhecker and Manias (2000) who first explored the PVOH/MMT nanocomposite.

Table 4.1: Crystallinity of neat PVOH – MMT blends

Sample	Enthalpy of melting (ΔH_m)	Crystallinity (%)
PM-1	55.33	34.37
PM-3	55.87	34.70
PM-5	59.56	36.99
PM-7	59.51	36.96
PM-9	53.94	33.50

4.2.2 Interaction of 50 % PVOH with various amount of MMT

From Figure 4.11, as the amount of MMT were increased from 0.1, 0.3, 0.5, 0.7 to 0.9 g, sample with 50 % of PVOH and 0.9 g of MMT showed higher enthalpy among all samples with 50 % PVOH which is about 32.54 J/g. The difference for this section compared to the previous section is the incorporation of 50 % of CRS. In this case, with 50 % of CRS incorporated, the enthalpy was seen to increase from 23.81 J/g to 32.54 J/g. When starch was added, the presence of hydroxyl groups tend to form strong bonding among all three different molecules and subsequently led to better system integrity with the addition of MMT up to 0.9 g. Thus, more energy was needed to break the bonding and releasing the polymer chains from its rigid crystal structure to reach melting point. Although there was strong bonding among the molecules, the samples containing starch compounds presented lower enthalpy of melting values compared to the neat PVOH-MMT blends. This indicates that the intermolecular bondings between PVOH-MMT molecules are much stronger compared to intermolecular bonding between PVOH-MMT-CRS.

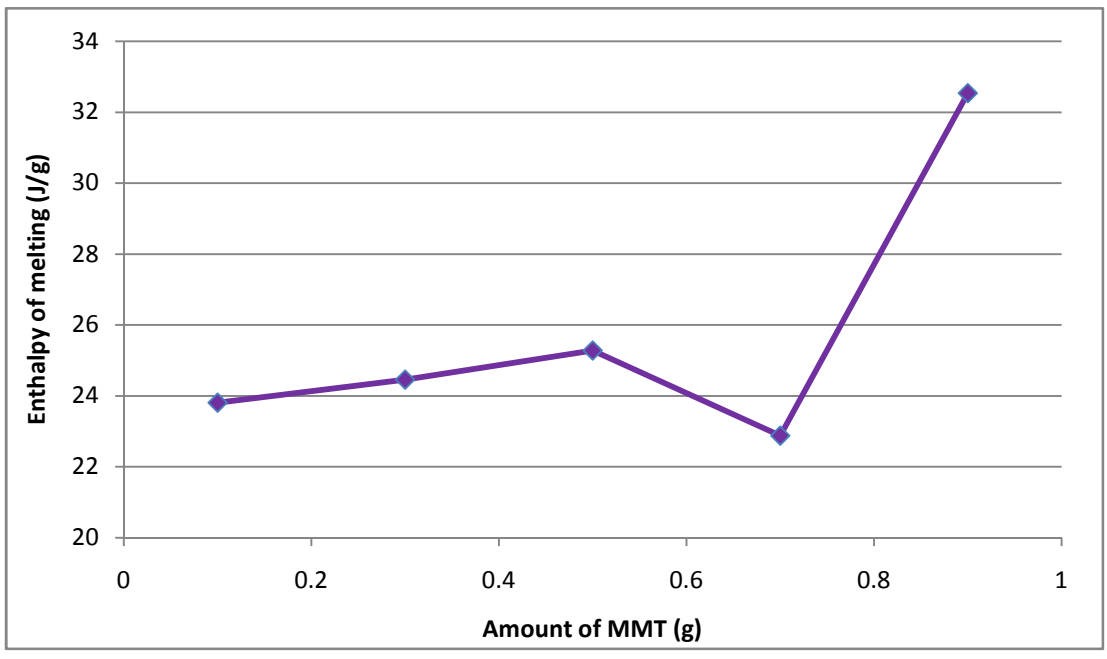

Figure 4.11: Enthalpy of melting of 50 % PVOH – MMT blends

Table 4.2 shows the nanocomposite crystallinity. From the table, it can be seen that, as the amount of MMT increases, the crystallinity (%) increases. This increase probably occurred due to the increase in ordered chain branching in the blend. The degree of branching on the main backbone might have decrease with the addition of MMT more than 0.1 g. Thus, the lowly branched system would eventually increase the crystallinity.

Table 4.2: Crystallinity of 50 % PVOH – MMT blends

Sample	Enthalpy of melting (ΔH_m)	Crystallinity (%)
PCM-55-1	23.81	14.79
PCM-55-3	24.46	15.19
PCM-55-5	25.28	15.70
PCM-55-7	22.88	14.21
PCM-55-9	32.54	20.21

4.2.3 Interaction of 0.1 g of MMT with various amount of PVOH

From Figure 4.12, as the amount of PVOH increases from 20 %, 30 %, 40 %, 50% and 100 % with 0.1 g of MMT, the enthalpy of melting increases proportionally. When the first 20 % of PVOH was incorporated with 80 % CRS and 0.1 g of MMT, the CRS portion which dominates tends to weaken the overall interaction of PVOH. The enthalpy of melting increases with the increasing amount of PVOH because there were extra physical bonding formations between PVOH – MMT - CRS. The enthalpy of melting then increased linearly with further addition of PVOH. The highest enthalpy of melting of 55.33 J/g was achieved when 100 % of PVOH was incorporated with 0.1 g of MMT. As explained above, this indicates that the physical bonding between PVOH – MMT are much stronger and better compared to physical bonding between PVOH – MMT - CRS blends. Thus, the energy needed to break the bonding and releasing the polymer chains from its rigid crystal structure to reach the melting stage.

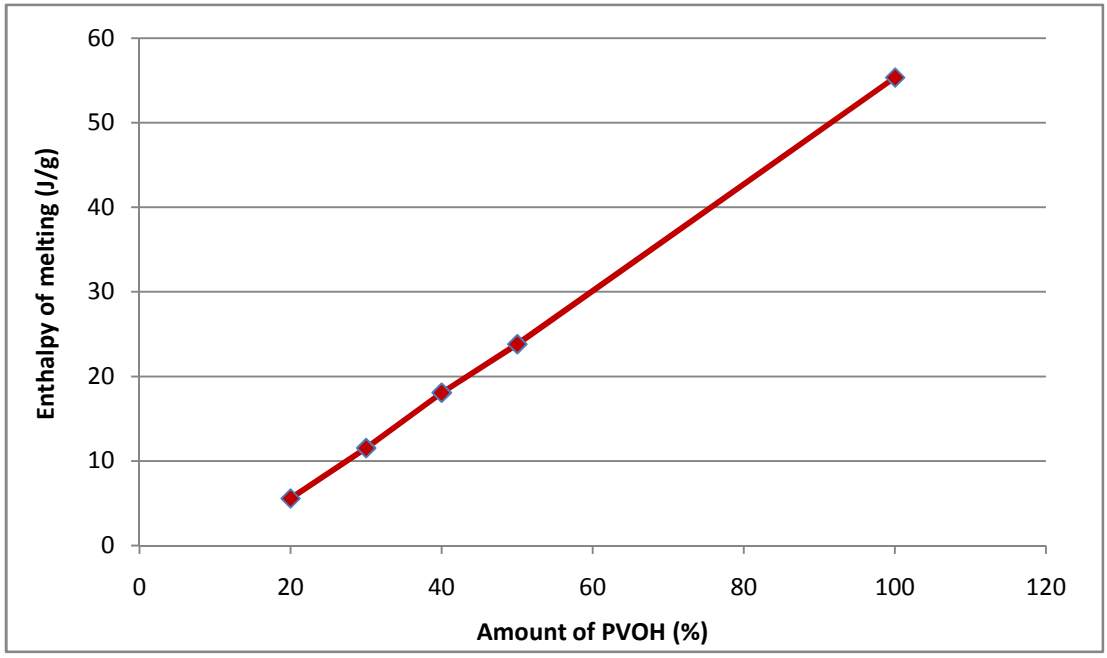

Figure 4.12: Enthalpy of melting of 0.1 g MMT – PVOH blends

From table 4.3, it can be clearly seen that the crystallinity increases proportionally with increasing amount of PVOH from 20 % to 100 %. As mentioned above, this increase probably occurred due to the increase in ordered chain branching in the blend. The degree of branching on the main backbone might have decrease with the addition of MMT more than 0.1 g. Thus, the lowly branched system would eventually increase the crystallinity.

Table 4.3: Crystallinity of 0.1 g MMT – PVOH blends

Sample	Enthalpy of melting (ΔH_m)	Crystallinity (%)
PCM-28-1	5.58	0.04
PCM-37-1	11.53	0.07
PCM-46-1	18.08	0.11
PCM-55-1	23.81	14.79
PM-1	55.33	34.37

4.3 Physical properties/ Morphologies (SEM)

4.3.1 Interaction of neat PVOH with various amount of MMT

Figure 4.13 shows the surface morphologies of 100 % PVOH with various amount of MMT observed using the Hitachi Scanning Electronic Microscopy of BS 340 TESLA. By comparing the SEM images in figure 4.13 (a) to (e), it can be clearly seen that the MMT particles was distributed evenly with very less agglomeration with the PVOH compound for the sample when the amount of MMT is 0.5 g. For low amount of MMT, the MMT particles were less and were not distributed all over the system. However as the amount of MMT increases to 0.9 g, both the compounds became more agglomerate with each and other. As discussed above, this would eventually decrease the tensile strength as MMT increases more than 0.5 g.

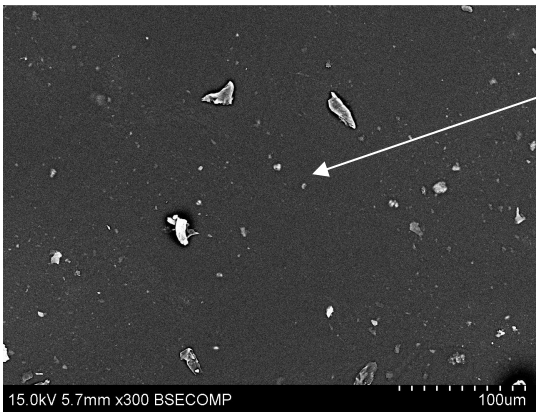

(a)

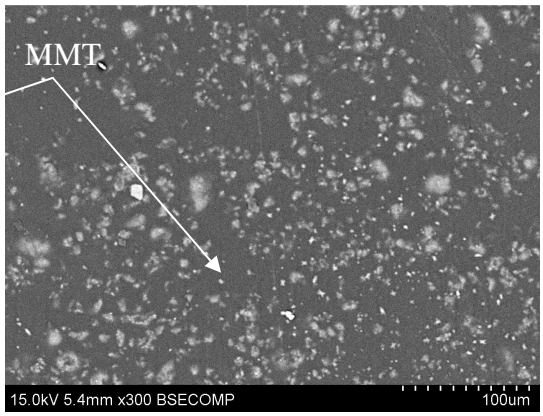

(b)

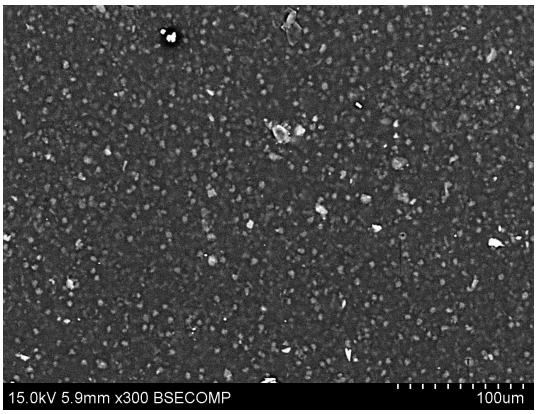

(c)

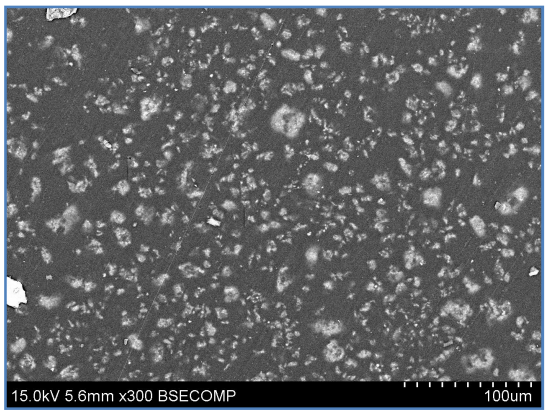

(d)

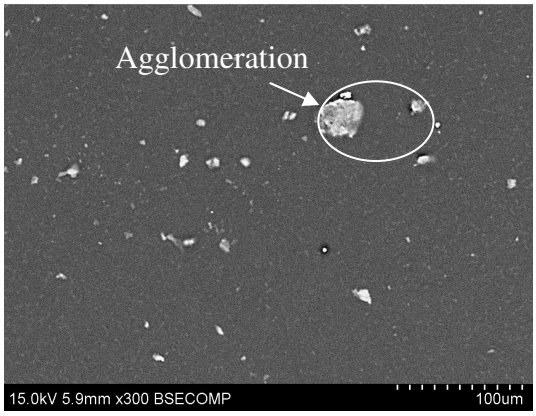

(e)

Figure 4.13: Surface morphology of 100 % PVOH with (a) 0.1 g MMT; (b) 0.3 g MMT; (c) 0.5 g MMT; (d) 0.7 g MMT; (e) 0.9 g MMT

4.3.2 Interaction of 50 % PVOH with various amount of MMT

Figure 4.14 shows the surface morphologies of 50 % PVOH with various amount of MMT observed using the Hitachi Scanning Electronic Microscopy of BS 340 TESLA. By comparing the SEM images in figure 4.14 (a) to (e), it can be observed that the MMT particles was distributed evenly when the amount of MMT incorporated was 0.9 g (e). However, for lower amount of MMT (0.1-0.5 g) incorporated, there was sign of intercalation observed, the SEM image showed an intercalated image between both the compounds. As mentioned above, this would eventually increase the tensile strength as MMT increases.

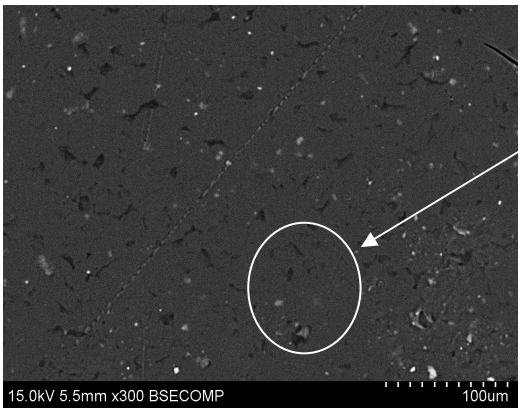

(a)

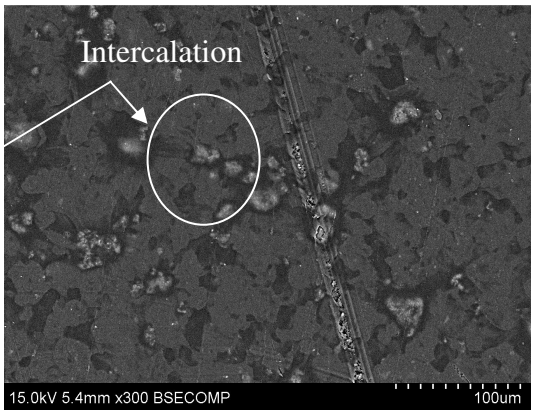

(b)

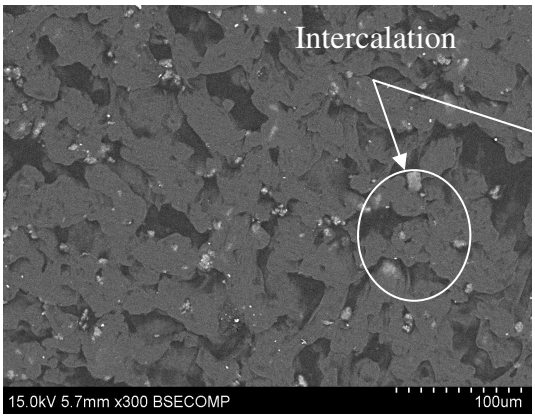

(c)

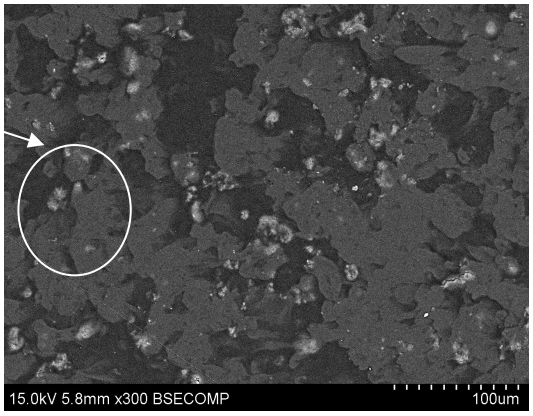

(d)

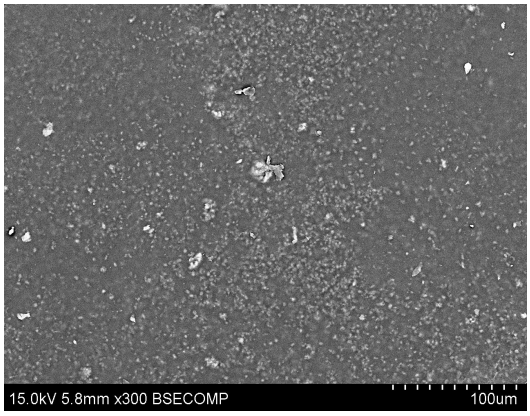

(e)

Figure 4.14: Surface morphology of 50 % PVOH with (a) 0.1 g MMT; (b) 0.3 g MMT; (c) 0.5 g MMT; (d) 0.7 g MMT; (e) 0.9 g MMT

4.3.3 Interaction of 0.1 g of MMT with various amount of PVOH

Figure 4.15 shows the surface morphologies of 0.1 g MMT with various amount of PVOH observed using the Hitachi Scanning Electronic Microscopy of BS 340 TESLA. From figure 4.15 (a) to (f), it can be observed that the MMT particles were seen to agglomerate when the amount of PVOH incorporated was 20 % (a) and 30 % (b). As the amount of PVOH reaches 40 % (c), the MMT particles are begin to distribute. As it reaches 50 % (d) of PVOH, the MMT was seen to be evenly distributed. This was the reason for the high tensile strength for sample with 50 % of PVOH and 0.5 g MMT. As the amount of PVOH were further increased to 100 % (e), the domination of PVOH causes intercalation between the compounds.

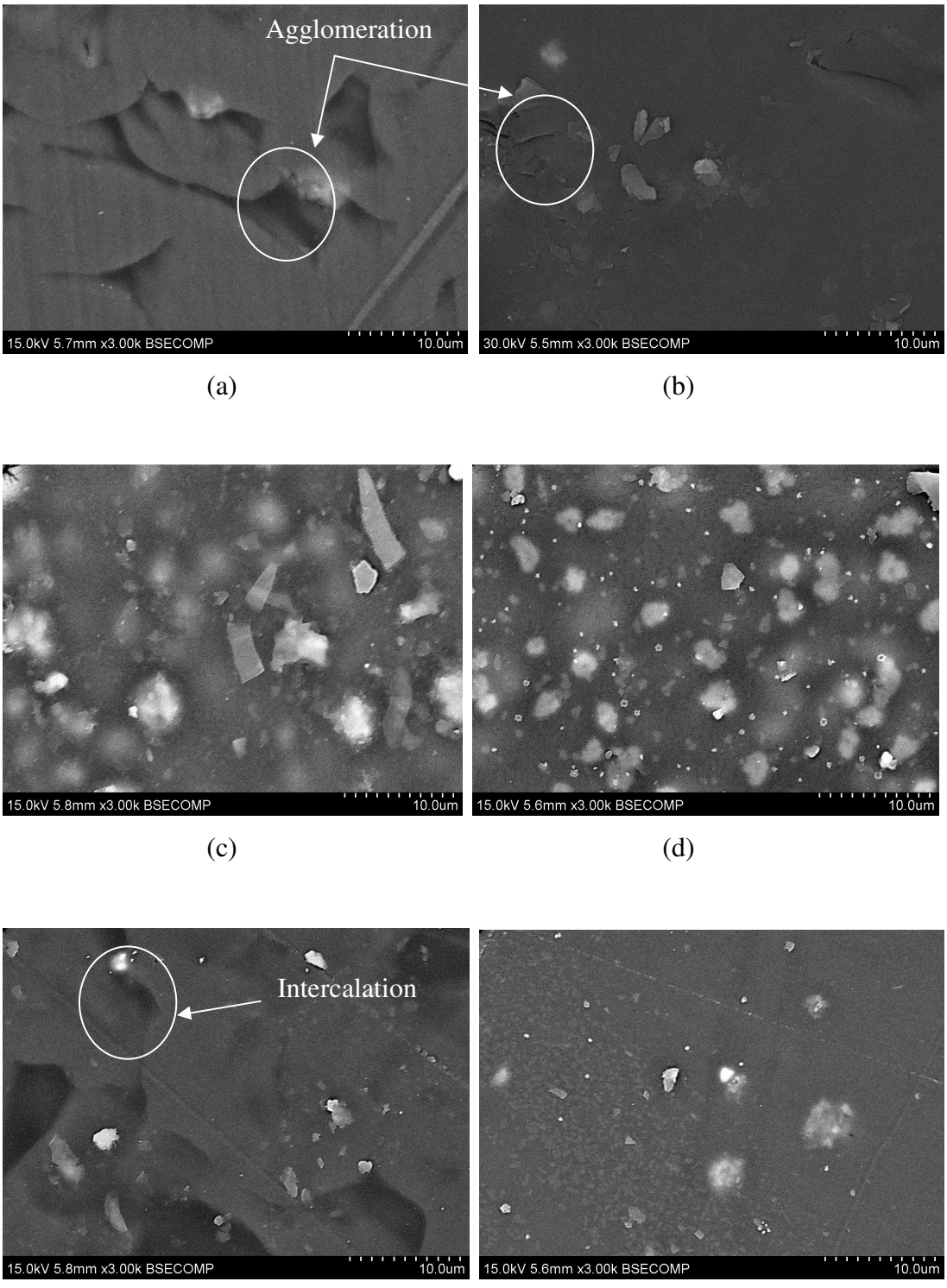

Figure 4.15: Surface morphology of 0.1 g MMT with (a) 20 % PVOH; (b) 30 % PVOH; (c) 40 % PVOH; (d) 50 % PVOH; (e) 100 % PVOH; (f) 100 % CRS

4.4 Interaction of bonding (FTIR)

4.4.1 Interaction of PVOH with various amount of MMT

Besides mechanical properties, thermal properties and physical properties, another important field also was studied in the evaluation of MMT on PVOH - CRS compound which is the interaction of bonding. As shown in figure 4.16, the O-H stretch characteristic peak was appeared to be higher for sample with 100 % PVOH and 0.5 g of MMT which is about 3469 cm^{-1}. This is because the intermolecular H-bonding between starches chains were disrupt by the high amount of PVOH.

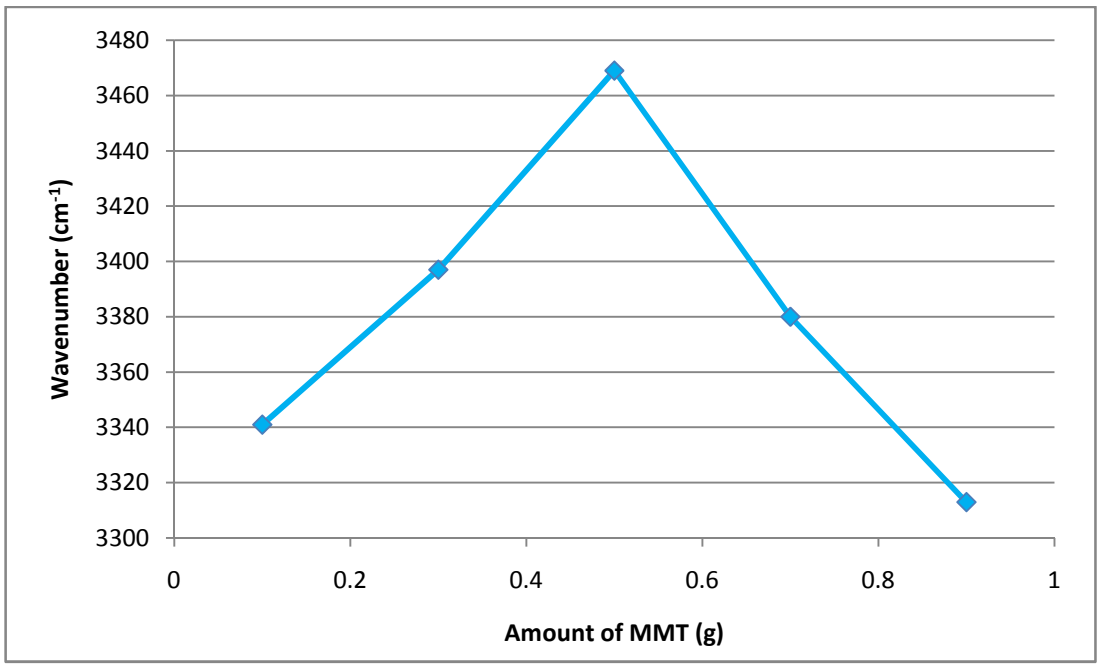

Figure 4.16: O-H stretch differences from FTIR for neat PVOH – MMT blends

Comparing all the samples with 50 % of PVOH, when the amount of PVOH and CRS were kept constant at 50 % and the amount of MMT increased, the O-H stretching shows a greater shift to a higher value. This shift can be clearly observed in the Figure 4.17 which is from 3392-3471 cm^{-1} when MMT used was increased from 0.3g – 0.9g. This is because, with further addition of MMT, the H-bonding between the PVOH and CRS was disrupted and this distruption of H-bonding led to a greater O-H bonding. However, the lowest O-H peak was observed at 3308 cm^{-1} which is when 0.1g of MMT was introduced in 20 % of PVOH. This result is also closely related to the previous explanation which is when the amount of CRS is higher, it lead to a stronger H-bonding thus disrupt the O-H bonding.

The characteristic vibration bands of PVA were clearly shown in the first group of samples where the amount of MMT increased from 0.1g to 0.9 g in 100 % of PVOH. This has been represented by the peak at 3313-3468 cm^{-1} (-OH), 2937-2943cm^{-1} (-CH3), 1435-1458 cm^{-1} (O=C-OR), 1094-1100 cm^{-1} (C- O -C), 859 cm^{-1} (CH).

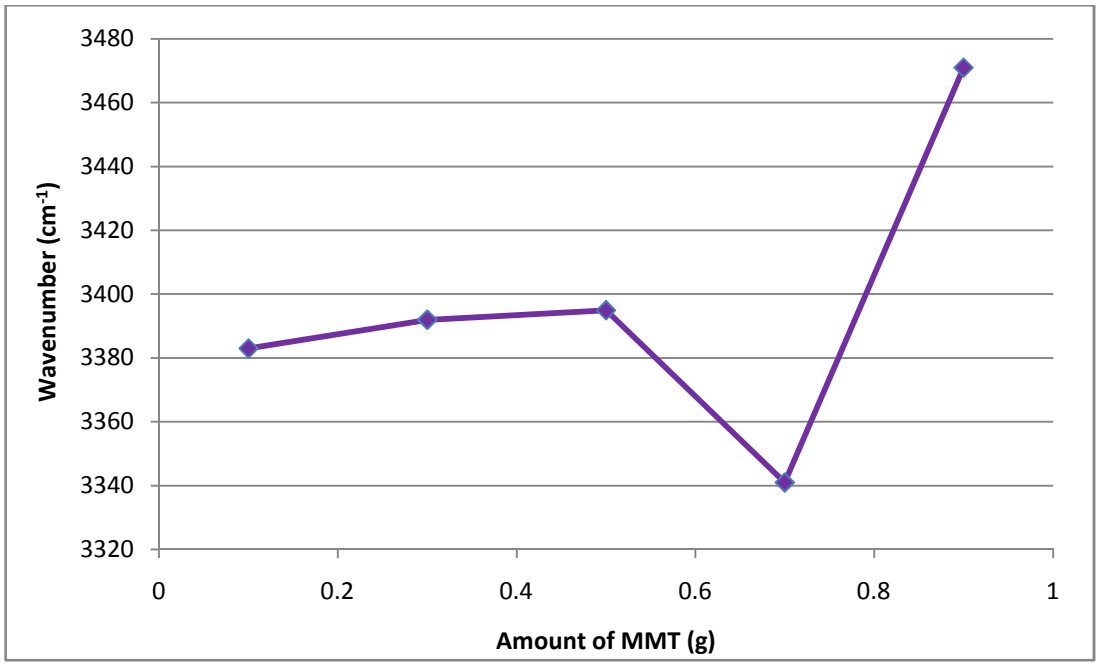

Figure 4.17: O-H stretch differences from FTIR for 50 % PVOH – MMT blends

4.4.2 Interaction of 0.1 g of MMT with various amount of PVOH

The interaction of bonding between PVOH and CRS was also studied carefully when the amount of MMT was kept constant at 0.1 g. Figure 4.18 below shows the O-H stretch differences from FTIR for 0.1 g MMT - PVOH blends. In general, the spectra for all specimens seem to present in almost similar absorption manners. A close inspection on the range of 3000-3500 cm^{-1} showed that increasing amount of PVOH from 20 % to 100 % by weight has shifted the O-H stretch in a fluctuating manner.

From Figure 4.18, the highest O-H stretch peak was for the sample with 50 % of PVOH and 0.1 g MMT. The strength of hydrogen bond in the sample is not only limited to chemical environment within the molecules but could also be affected by other physical environment such as crystalline and amorphous structure (He, Zhu & Inoue, 2004). A crystal structure will cause a higher shifting of absorption spectra due to the extra energy required to overcome vibration or stretching in a constraint structure (Sin et al., 2010).

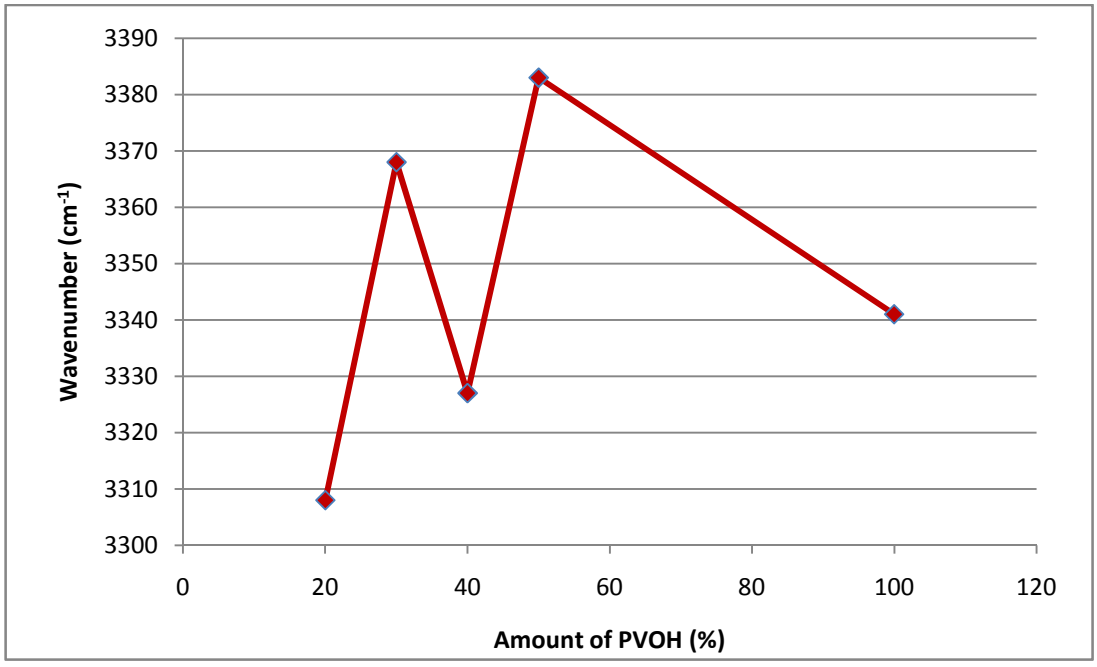

Figure 4.18: O-H stretch differences from FTIR for 0.1 g MMT - PVOH blends

Basically addition of PVOH to corn starch prevented the development of surface cracks, indicating relatively good compatibility of corn starch and PVOH. Because both corn starch and PVOH are polar substances having hydroxyl groups (-OH) in their chemical structure, these highly polar hydroxyl groups tend to form intermolecular and intramolecular hydrogen bonds which improve the integrity of corn starch–PVOH blends

CHAPTER 5

CONCLUSION AND RECOMMENDATION

5.1 Conclusion

This study has evaluated the characteristics of the polyvinyl alcohol (PVOH) – corn starch (CRS) compound and their corresponding interactions with montmorillonite (MMT) compound. Following are the conclusion made from this study:

5.1.1 Mechanical properties

For samples with neat PVOH, as the amount of MMT increases, the tensile strength increases from 1.3 MPa to 16.0 MPa and further addition above 0.5 g of MMT decreases the tensile strength to 10.7 MPa. The percentage elongation at break showed similar trend with increase of elongation from 25.4 % to 82.7 % and decreases to 53.7 MPa. The modulus increased from 48.7 MPa to 86.5 MPa.

For samples with 50 % of PVOH, as the amount of MMT increases, the tensile strength increases from 20.6 MPa to 27.1 MPa. The percentage elongation at break showed similar trend with increase of elongation from 9.2 % to 12.3 %. The modulus was also seen to increase from 584.5 MPa to 742.3 MPa.

For samples with 0.1 g of MMT, as the amount of PVOH increases, the tensile strength increases from 2.5 MPa to 20.6 MPa and decreased to 1.3 MPa for further addition of PVOH. The percentage elongation at break increases from 3.6 % to 25.4 %. The modulus was seen to increase from 130 MPa to 1259 MPa and decreased to 48.7 MPa for further addition of MMT. These results indicate that addition of MMT only up to 0.5 g in 50 % of PVOH possesses the highest mechanical properties.

5.1.2. Thermal properties

For samples with neat PVOH, as the amount of MMT increases, the enthalpy of melting (ΔH_m) increases from 55.33 J/g to 59.56 J/g and decreases to 53.94 J/g for further addition of MMT. The crystallinity showed similar trend where it increases from 34.37 % to 36.99 % and decreases to 33.50 % for further addition of MMT.

For the samples with 50 % PVOH, as the amount of MMT increases, the enthalpy of melting (ΔH_m) increases from 23.81 J/g to 32.54 J/g. The crystallinity showed similar trend where it increases from 14.79 % to 20.21 %.

For the samples with 0.1 g of MMT, as the amount of PVOH increases, the enthalpy of melting (ΔH_m) increases from 5.58 J/g to 59.56 J/g. The crystallinity showed similar trend where it increases from 0.04 % to 34.37 %. These results indicate that addition of MMT only up to 0.5 g in neat PVOH possesses highest thermal stability.

5.1.3. Interaction of bonding

For sample with neat PVOH, when the amount of MMT increases, the O-H stretch characteristic peak shifted higher from 3341 cm^{-1} to 3469 cm^{-1} and shifted lower to 3313 cm^{-1}.

For sample with 50 % PVOH, when the amount of MMT increases, the O-H stretch characteristic peak shifted higher from 3383 cm^{-1} to 3471 cm^{-1}.

For sample with 0.1 g of MMT, when the amount of MMT increases, the O-H stretch characteristic peak shifted higher from 3308 cm^{-1} to 3383 cm^{-1} and shifted lower to 3341 cm^{-1}. These results indicated that addition of 0.9 g MMT into 50 % PVOH possesses strongest interaction of bonding between molecules.

5.1.4. Physical properties/ Morphologies

Scanning Electron Microscopy (SEM) results indicated that, MMT particles are well distributed when 0.5 g of MMT was incorporated with neat PVOH and further addition of MMT causes agglomeration between molecules. For samples with 50 % PVOH, MMT loadings of 0.9 g showed even better distribution compared to the neat PVOH sample. When MMT is kept constant at 0.1 g, the sample with 50 % PVOH showed well distributed particles.

5.2 Recommendations

It is recommended that another analysis using X-Ray Diffraction (XRD) is carried out in this research. This will be useful to evidence the presence of another crystal phase in the nanocomposite with the addition of nano-sized MMT. Besides, Thermogravimetric analysis (TGA) should also needed in this research to evidence the thermal stabilities in detail.

REFERENCES

Alexandre, M., & Dubois, P. (2000). Polymer-layered silicate nanocomposites: preparation, properties and uses of a new class of materials. *Material Science and Engineering, 28*, 1-63.

Antoniassi, R., Esteves, W., & Meirelles, A.J.A. (1998). Pretreatment of corn oil for physical refining. *Journal of the American Oil Chemists Society, 75*, 1411-1415.

Aracil, I., Font, R., Conesa, J. A., & Fullana, A. (2007). TG-MS analysis of the thermo-oxidative decomposition of polychloroprene. *Journal of Anaytical and Applied. Pyrolysis, 79*, 327-336.

Ashish V., Mohod, Parag, R., & Gogate. (2011). Ultrasonic degradation of polymers: Effect of operating parameters and intensification using additives for carboxymethyl cellulose (CMC) and polyvinyl alcohol (PVA). *Ultrasonics Sonochemistry, 18*, 727-734.

Avella, M., Bondioli, F., Canillo, V., DiPace, E., Errico, M.E., Ferrari, A.M., Focher, B., & Malinconico, M. (2006). Poly(ε-caprolactone)-based nanocomposites: influence of compatibilization on properties of poly(ε-caprolactone)-silica nanocomposites. *Composites Science and Technology*, 66, 886-894.

Avella, M., Carfagna, C., Cerruti, P., Ericco, M. E., & Gentile, G. (2006). Nylon based nanocomposites : influence of calcium carbonate nanoparticles on the thermal stability. *Macromolecular Symposia, 234*, 163-169.

Babel, S., & Kurniawan, T.A. (2003). Low-cost adsorbents for heavy metals uptake from contaminated water: A review. *Journal of Hazardous Materials, 97 (1-3),* 129-243.

Baldassari, S., Komarneni, S., Mariani, E., & Villa, C., (2006). Microwave versus conventional preparation of organoclays from natural and synthetic clays. *Applied Clay Science, 31, (1-2)*, 134-141.

Blaine, R.L. (1990). Thermal Application Notes*, Polymers Heats of Fusion*, TA Instruments, 109 Lukens Drive, New Castle DE 19720, USA.

Bertini, F. Canetti, M. Audisio, G. Costa, G. Falqui, L., (2006). Characterization and thermal degradation of polypropylene montmorillonite nanocomposites. *Polymer Degradation and Stability*, (91), 1929-1936.

Bondar, D., (2009). Alkali activation of Iranian natural pozzolans for producing geopolymer cement and concrete. A dissertation submitted to University of Sheffield in fulfilment of the requirements for the degree of Doctor of Philosophy, U.K.

Botana, A., Mollo, M., Eisenberg, Patricia., Torres Sanchez, R.M. (2010). Effect of modified montmorillonite on biodegradable PHB nanocomposites. *Applied Clay Science, 47*, 263-270.

Botines, E., & Puiggali, J. (2006). Crystallization kinetics of poly (glycolic acid-alt-6-aminohexanoic acid). *European Polymer Journal, 42*, 1595-1608.

Bourbigot, S. Gilman, J.W., & Wilkie, C.A., (2004). Kinetic analysis of the thermal degradation of polystyrene-montmorillonite nanocomposite. *Polymer Degradation and Stability, 84 (2)*, 483-492.

Boz, E. Nemeth, A. J., Ghiviriga, I., Jeon, K., Alamo, R. G., & Wagener, K. B. (2007). Precision ethylene/vinyl chloride polymers via condensation polymerization. *Macromolecules, 40*, 6545-6551.

Bras. A. R., Viciosa, M.T., Wang, Y. M., Dionisio, M., & Mano, J. F. (2006). Crsytalization of poly(L-lactic acid) probed with dielectric relaxation spectroscopy. *Macromolecules, 39*, 6513-6120.

Braun, U., Balabanovich, A. I., Schartel, B., Knoll, U., Artner. J., Ciesielski, M., Doring, M., Perez, R., Perez, R., Sandler, J. K. W., Altstadt, V., Hoffmann, T., & Pospiech, D. (2006). Influence of the oxidation state of phosphorus on the decomposition and fire behaviour of flame-retarded epoxy resin composites. *Polymer, 47*, 8495-8508.

Brindley, G.W., & Radoslovich, W.W. (1956). X-ray study of the alteration of soda feldspar. *Clays Clay Minerals*, Vol (4), National Academy of Science, Washington, DC.

Bruno, M., Prencipe, M., & Valdre, G., (2006). Ab initio quantum-mechanical modelling of pyrophyllite [Al2Si4O10(OH)2] and talc [Mg3Si4O10(OH)2] surfaces. *Physics and Chemistry of Mineral, 33 (1)*, 63-71.

Cai, J. L., Li, T., Han, Y., Zhuang, Y. Q., & Zhang, X. Q. (2006). Nonisothermal crystallization kinetics and morphology of self-seeded syndiotactic 1,2-polybutadiene. *Journal of Applied Polymer Science, 100*, 1479-1491.

Cai, Y. Huang, F., Xia, X., Wei, Q., Tong, X., & Wei, A. Gao, W. (2010). Comparison between structures and properties of ABS nanocomposites derived from two different kinds of OMT. *Journal of Materials Engineering Performance, 19*, 171-176.

Cai, Z.Q., Sun, J. Z., Wang, D. D., & Zhou, Q.Y. (2007). Studies on curing kinetics of a novel combined liquid crystalline epoxy containing tetramethylbiphenyl and aromatic ester-type mesogenic group with diaminodiphenylsulfone. *Journal of Polymer Science, Part A: Polymer Chemistry, 45*, 3922-3928.

Cerda, M.A., Luengas, G., Navarrete, M.A., Sanchez, E., & Guzman, J. (2003). Elastic and burning properties of PVA/MMT nanocomposites. Universidad Nacional Autonoma de Mexico, Instituto de Investigaciones en Materiales, C.P. 04510, Coyoacan, D.F., Mexico.

Cervellera, R., Ramis, X., Salla, J. M., Mantecom, A., & Serra, A. (2007). Kinetics study of the curing of mixture of DGEBA and five-membered cyclic carbonates with lanthanum triflate as cationic initiator. *Journal of Applied Polymer Science, 103*, 2875-2884.

Chartoff, R.J. (2006). Thermal characteristics of thermosets formed by free radical photocuring. *Journal of Thermal Analysis and Calorimetry, 85*, 213-217.

Chen, Y., Cao, X., Chang, P. R., Huneault, M. A. (2008). Comparative study on the films of poly(vinyl alcohol)/pea starch nanocrystals and poly(vinyl alcohol)/native pea starch. *Carbohydrate Polymers, 73*, 8–17.

Chen, K., Harris, K., & Vyazovkin, S. (2007). Tacticity as a factor contributing to the thermal stability of polystyrene. *Macromolecular Chemistry and Physics, 208*, 2525-2532.

Chen, K., Wilkie, C. C., & Vyazovkin, S. (2007). Nanoconfinenment revealed in degradation and relaation studies of two structurally different polystyrene-clay systems. *Journal of Physcal Chemistry, 111*, 12685-12692.

Chiellini, E., Corti, A., D'Antone, S., & Solaro, R. (2003). Biodegradation of poly (vinyl alcohol) based materials. *Progress in Polymer Science 2003, 28 (6)*, 963–1014.

Chieng, B.W., Ibrahim, N. A., & Wan Yunus W. M. Z. (2010). Effect of organo-modified montmorillonite on poly(butylene succinate)/poly(butylene adipate-co-terephthalate) nanocomposites. *eXPRESS Polymer Letters, (4)*, 404-414.

Chigwada, G. Wang, D. Jiang, D.D., & Wilkie, C.A., (2006). Styrenic Nanocomposites prepared using a novel biphenyl-containing modified clay. *Polymer Degradation and Stability*, 91, 755-762

Chivrac, F., Pollet, E., & Luc Averous. (2009). Progress in nano-biocomposites based on polysaccharides and nanoclays. *Material Science and Engineering R 67*, 1-17.

Choi, Y.S. Xu, M.Z., & Chung, I.J. (2005). Synthesis of exfoliated acrylonitrile butadiene–styrene copolymer (ABS) clay nanocomposites: role of clay as a colloidal stabilizer. *Polymer, 46*, 531-538.

Chow, W.S., & Tham, W.L. (2009). Thermal and antistatic properties of polypropylene/ organo montmorillonite nanocomposites. Polymer–*Plastics Technology and Engineering, 48*, 342-350.

Choy, J.H., Choi, S.J., Oh, J.M., & Park, T. (2007). Clay minerals and layered double hydroxides for novel biological applications. *Applied Clay Science, 36*, 122-132.

Chrissafis, K., & Bikiaris, D. (2011). Review: Can nanoparticles really enhance thermal stability of polymers? Part I: An overview on thermal decomposition of addition polymers. *Thermochimica Acta, 523*, 1-24.

Chrissafis, K. Paraskevopoulos, K.M. Papageorgiou, G.Z., & Bikiaris, D.N. (2008). Thermal and dynamic mechanical behavior of bionanocomposites: fumed silica nanoparticles dispersed in poly(vinyl pyrrolidone), chitosan, and poly(vinyl). *Journal of Applied Polymer Science, 110*, 1739-1749.

Chrissafis, K. Paraskevopoulos, K.M. Pavlidou, E., & Bikiaris, D. (2009). Thermal degradation mechanism of HDPE nanocomposites containing fumed silica nanoparticles. *Thermochimica Acta, 485*, 65-71.

Chrissafis, K. Paraskevopoulos, K.M. Tsiaoussis, I., & Bikiaris, D. (2009). Comparative study of the effect of different nanoparticles on the mechanical properties, permeability, and thermal degradation mechanism of HDPE. *Journal of Applied Polymer Science, 114*, 1606-1618.

Chrissafis, K., Antoniadis, G., Paraskevopoulos, K. M., Vassiliou, A., & Bikiaris, D. N, (2007). Clay dispersion in polyethylene/clay nanocomposites. *Composites Science and Technology, 67*, 2165-2174.

Chuayjuljit, S., Hosililak, S., &. Athisart, A. (2009). Thermoplastic Cassava Starch/Sorbitol-Modified Montmorillonite nanocomposites blended with Low Density Polyethylene: Properties and biodegradability study. *Journal of Metals, Materials and Minerals, (19),* 59-65.

Constantin, M., Fundueanu, G., Bortolotti, F., Cortesi, R., Ascenzi, P., & Menegatti, E. (2004). Preparation and characterisation of poly (vinyl alcohol)/ cyclodextrin microspheres as matrix for inclusion and separation of drugs. *International Journal of Pharmaceutics, 285 (1-2),* 87-96.

Costa, F.R., Wagenknecht, U., & Heinrich, U. (2007). LDPE/Mg-Al layered double hydroxide nanocomposite: thermal and flammability properties. *Polymer Degradation and Stability, 92*, 1813-1823.

Costache, M. C. Heidecker, M.J. Manias, E. Camino, G. Frache, A. Beyer, G. Gupta, R. K. Wilkie, C., (2007). The influence of carbon nanotubes, organically modified montmorillonite and layered dounble hydroxides on thermal degradation and fire retardancy of polyethylene, ethylene-vinyl acetate copolymer and polystyrene. *Polymer, 48*, 6532-6545.

Costache, M.C., Jiang, D.D., & Wilkie, C.A. (2005). Thermal degradation of ethylene–vinyl acetate copolymer nanocomposites. *Polymer, 46*, 6947-6958.

Davidovits J. (1994). Geopolymers, man-made rock geosynthesis and the resulting development of very early high strength cement. Journal of Materials Education, 16, 91-137.

Dean, K. M., Do, M. D., Petinakis, E., & Yu, L. (2008). Key interactions in biodegradable thermoplastic starch/poly(vinyl alcohol)/montmorillonite micro- and nanocomposites. *Composites Science and Technology, 68(6),* 1453–1462.

DeMerlis, C.C., & Schoneker, D.R. (2003). Review of the oral toxicity of polyvinyl alcohol (PVA). *Food and Chemical Toxicology, 41*,319-326.

DiGianni, A. Ameri, E. Monticell, O. Bongiovanni R., (2008). Preparation of polymer/clay mineral nanocomposites via dispersion of silylated montmorillonite in a UV curable epoxy matrix. *Applied Clay Science, 42*, 116-124.

DiLorenzo, M. L. Sajkiewicz, P. La Pietra, P. Gradys, A., (2006). Irregularly shaped DSC exotherms in the analysis of polymer crsytallization. *Polymer Bulletin, 57*, 713-21.

Dzunuzovic, E., Jeremic, K., & Nedeljkovic, J. M. (2007). In situ radical polymerization of methyl methacrylate in a solution of surface modified TiO_2 and nanoparticles. *European Polymer Journal, 43*, 3719-3726.

Erickson, K. L. (2007). Thermal decomposition mechanisms common to polyurethane, epoxy, poly (diallyl phthalate), polycarbonate and poly(phenylene sulfide). *Journal of Thermal Analysis and Calorimetry, 89*, 427-440.

Essawy, H.A. Badran, A.S. Youssef, A.M. El-Fettouh, A., & El-Hakim, A.A. (2004). Polystyrene/montmorillonite nanocomposites prepared by in situ intercalative polymerization: influence of the surfactant type. *Macromolecular Chemistry and Physics, 205*, 2366-2370.

Fornes, T., Yoon, P., & Paul, D. (2003). Polymer matrix degradation and colour formation in melt processed nylon 6/clay nanocomposites. *Polymer,44*, 7545-7556.

Fujihara, K., Kotaki, M., & Ramakrishna, S. (2005). Guided bone regeneration membrane made of polycaprolactione/calcium carbonate composite nano-fibers. *Biomaterials 26*, 4139-4147.

Fukushima, H. T., Drzal, L., Rook, B. P., Rich, M. J. (2006). Thermal conductivity of exfoliated graphite nanocomposites. *Journal of Thermal Analysis and Calorimetry, 85*, 235-238.

Garcia, N. Hoyos, M. Guzman, M. Tiemblo, P. (2009). Comparing the effect of nanofillers as thermal stabilizers in low density polyethylene.

Garrido-Ramirez, E.G., Theng, B.K.G., & Mora, M.L. (2010). A Review Article: Clays and oxide minerals as catalysts and nanocatalysts in Fenton-like Reactions. *Applied Clay Science, 47*, 182-192.

Giannakas, A., Xidas, P., Triantafyllidis, K.S., Katsoulidis, A., & Ladavos A., (2009). Preparation and characterization of polymer/organosilicate nanocomposites based on unmodified LDPE. *Journal of Applied Polymer Science, 114*, 83-89.

Gupta, V., & Rastogi, A. (2008). Biosorption of lead (II) from aqueous solutions by nonliving algal biomass Oedogonium sp. and Nostoc sp. A comparative study. *Journal of Hazardous Materials, 152*, 407-414.

Hablot, E., Bordes, P., Pollet, E., & Avérous, L. (2008). Thermal and thermo-mechanical degradation of poly (3-hydroxybutyrate)-based multiphase systems. *Polymer Degradation and Stability, 93*,413-421.

Hargis, M., Grady, B.P., Aktas, L., Bomireddy, K. R., Howsman, S., Altan, M. C., Rose, T., & Rose, H. (2006). Calorimetric and rheological measurements of three commercial thermosetting prepreg epoxies. *Journal of Composite Materials, 40*, 873-897.

Hargis, M. J., & Grady, B. P. (2006). Effect of sample size on isothermal crystallization measurement performed in a DSC : A method to determine avrami parameters without sample thickness effects. *Thermochimica Acta, 443*, 147-158.

Hartley, W. Edwards, R., & Lepp, N.W. (2004). Arsenic and heavy metal mobility in iron oxide-amended contaminated soils as evaluated by short- and long-term leaching tests. *Environmental Pollution, 131*, 495-504.

Hassan, M.S., & Abdel-Khalek, N.A., (1998). Beneficiation and applications of an Egyptian bentonite. *Applied Clay Science, 13*, 99-115.

Hatakeyama, H. Onishi, T. Endo, & T. Hatakeyama, T. (2007). Gelatin of chemically cross-linked methylcellulose studied by DSC and AFM . *Carbohydrate Polymers*, 69, 792-798.

Haurie, L., Fernandez A.I., & Velasco, J.I. (2007). Thermal stability and flame retardancy of LDPE/EVA blends filled with synthetic hydromagnesite/aluminium hydroxide/montmorillonite and magnesium hydroxide/aluminium hydroxide/ montmorillonite mixtures. *Polymer Degradation and Stability, 92*, 1082-1087.

He, A., Wang, L., Yao, W., Huang, B., Wang, D., & Han C.C. (2010). Structural Design of imidazolium and its application in PP/montmorillonite nanocomposites. *Polymer Degradation and Stability, 95 (4),* 651-655.

Hedley, C.B. Yuan, G. G, B.K., (2007).Thermal analysis of montmorillonites modified with quaternary phosphonium and ammonium surfactants. *Applied Clay Science, 35*, 80-188.

He, G.B., & Yan, N. (2007). Curing kinetics of polymeric diphenylmethane with different wood species. *International Journal of Adhesion and Adhesives, 27*, 244-249.

He, Y., Zhu, B., & Inoue, Y. (2004). Hydrogen bonds in polymer blends. *Progress in Polymer Science. (29)*, 1021-51

Hernandez, M., Dupuy, J., Duchet, J., & Sautereau, H. (2007). Kinetics modelling of the reaction for an Epoxy/PMMA/MMT ternary system. *Epoxy Polymers.* AR 102.

Homminga, D., Goderis, B., Hoffman, S., Reynaers, H., & Groeninckx, G. (2005). Influence of shear flow on the preparation of polymer layered silicate nanocomposites. *Polymer, 46*, 9941-9954.

Howell, B. A., & Uzibor, J. (2006). Thermal stability of poly (styrene) containing phosphorus in the mainchain. *Journal of Thermal Analysis and Calorimetry, 85*, 45-51.

Howell, B.A. (2007). Thermal properties of compounds possessing both solid-phase and gas-phase flame retardant potential. *Journal of Thermal Analysis and Calorimetry, 89*, 373-377.

Huang, M., Yu, J., & Ma, X. (2006). High mechanical performance MMT-urea and formamide-plasticized thermoplastic cornstarch biodegradable nanocomposites. *Carbohydrate Polymers, 3 (3),* 393–399.

Ishikawa, F., Murano, M., Hiraishi, M., Yamaguchi, T., Tamai, I., & Tsuji, A., (2002). Insoluble powder formulation as an effective nasal drug delivery system. *Pharmaceutical Research, 19*, 1097-1104.

Ismail, H., & Munusamy, Y. (2007). Polyvinyl Chloride/Organoclay Nanocomposite: Effects of filler loading and Maleic Anhydride. *Journal of Reinforced Plastic Composites, 26*, 1681.

Jaffe, M., Collins, G., & Menczel, J. (2006). The thermal analysis of fibers in the twenty first century : from textile, industrial and composite to nano, bio and multifunctional. *Thermochimica Acta*, 442, 95-99.

Jain, V.P., Proctor, A.,(2007). Production of conjugated linoleic acid-rich potato chips. *Journal of Food Science, 72 (1)*, 75-78.

Jang, L.W., Kang, C.M., & Lee, D.C. (2001). A new hybrid nanocomposite prepared by emulsion copolymerization of ABS in the presence of clay. *Journal of Polymer Science Part B: Polymer Physics, 39*, 719-727.

Jeong, K. U., Knapp, B. S., Ge, J. J., Graham, M. J., Tu, Y. F., Leng, S.W., Xiong, H. M., Harris, F. W., Cheng, S. Z. D. (2006). Structures and phase transformation of odd-numbered asymmetric main-chain liquid crystalline polyesters. *Polymer, 47*, 3351-3362.

Jia, Y. T., Gong, J., Gu, X. H., Kim, H. Y., Dong, J., & Shen, X. Y. (2007). Fabrication and characterization of poly (vinyl alcohol)/ chitosan blend nanofibers produced by electrospinning method. *Carbohydrate Polymers, 67*, 403-409.

Kaczmarek, H., & Podgorski, A. (2007). The effect of UV-irradiation on poly(vinyl alcohol) composites with montmorillonite. J*ournal of Photochemistry and Photobiology, A: Chemistry,191*, 209-215.

Kampeerapappun, P., Aht-ong, D., Pentrakoon, D., & Srikulkit, K. (2007). Preparation of cassava starch/montmorillonite composite film. *Carbohydrate Polymers 2007, 67 (2)*,155–63.

Kandare, E., Deng, H. M., Wang, D. Y., & Hossenlopp, J. M. (2006). Thermal stability and degradation of poly (methyl methacrylate)/ layered copper hydroxyl methacrylate composites. *Polymer for Advanced Technologies, 17*, 312-319.

Karadag, D., Koc, Y., Turan, M., & Armagan, B. (2006). Removal of ammonium ion from aqueous solution using natural Turkish clinoptilolite. *Journal of Hazardous Materials ,136*, 604–609.

Kawee Srikulkit., (2007). Preparation of cassava starch/montmorillonite composite film. *Carbohydrate Polymers, 67*, 155-163.

Kelly, C. M., DeMerlis, C. C., Schoneker, D. R., & Borzelleca, J. F. (2003). Subchronic toxicity study in rats and genotoxicity tests with polyvinyl alcohol. *Food and Chemical Toxicology, 41*, 719-727.

Khan, M.A,. Bhattacharia, S.K., Kader, M.A., & Bahari, K. (2006). Preparation and characterization of ultra violet (UV) radiation cured bio-degradable films of sago starch/PVA blend. *Carbohydrate Polymers, 63*, 500-506.

.

Kocaoba, S., Orhan, Y., & Akyüz, T. (2007). Kinetics and equilibrium studies of heavy metal ions removalby use of natural zeolite. *Desalination, 214*, 1-10.

Koh, Y.P., McKenna, G. B., & Simon, S. L. (2006). Calorimetric glass transition temperature and absolute heat capacity of polystyrene ultrathin films. *Journal of Polymer Science Part B: Polymer Physics, 44*, 3518-3527.

Krkljes, A. N., Marinovic- Cincovic, M. T., Kacarevic- Popovic, Z. M., & Nedeljkovic, J. M. (2007). Dynamic thermogravemetric degradation of gamma radiolytically synthesized Ag-PVA nanocomposite. *J. M. Thermochimica Acta, 460*, 28-34.

Kuljanin, J. Comor, M.I., Djokovic, V., & Nedeljkovic, J.M. (2006). Synthesis and characterization of nanocomposite of polyvinyl alcohol and lead sulfide nanoparticles. *Materials Chemisrty and Physics, 95*, 67-71.

Lee, E.M., Oh, Y.S., Ha, H.S., Jeong, H.M., & Kim, B.K. (2009). Ultra high molecular weight polyethylene/organoclay hybrid nanocomposites. Journal of *Applied Polymer Science, 114*, 1529-1534.

Li,H., Yu, Y., & Yang Y. (2005).Synthesis of exfoliated polystyrene/montmorillonite nanocomposite by emulsion polymerization using zwitterions as the clay modifier. European Polymer Journal, 41, 2016-2022.

Liu, H., Xie, F., Yu, L., Chen, L., &. Li, L. (2009). Thermal processing of starch-based polymers. *Progress in Polymer Science, 34*, 1348-1368.

Lorenzo, A. T., Arnal, M. L., Albuerne, J., & Muller, A. (2007). DSC isothermal polymer crystallization kinetics measurements and the use of the Avrami equation to fit data : Guidlines to avoid common problems. *Polymer Testing, 26*, 222-231.

Ma, H., Tong, L., Xu, Z., & Fang, Z. (2008). Intumescent flame retardant-montmorillonite synergism in ABS nanocomposites. *Applied Clay Science, 42*, 238-245.

Madbouly, S. A., & Otaigbe, J. U. (2006). Kinetics analysis of fractal gel formation in waterborne polyurethane dispersions undergoing high deformation flows. *Macromolecules, 39*,4144-4151.

Ibrahim, M.M., El-Zawawy, W.K., & Nassar, M.A (2010). Synthesis and characterization of polyvinyl alcohol/nanospherical cellulose particle films. *Carbohydrate Polymers, 79*, 694-699.

Majdzadeh-Ardakani, K., & Nazari, B. (2010). Improving the mechanical properties of thermoplastic starch/poly(vinyl alcohol)/clay nanocomposites. *Composites Science and Technology, 70*, 1557–1563.

Mamleev, V., Bourbigot, S., & Yvon, J. (2007). Kinetics analysis of thermal decomposition of cellulose : The main mass loss. *Journal of Analytical and Applied Pyrolysis, 80*, 151-165.

Mihai, P., Pauly, T.R., & Pinnavaia, T.J. (2000). Acidic porous clay heterostructures (PCH): Intragallery assembly of mesoporous silica in synthetic saponite clays. *Chemistry of Materials, 12 (9)*, 2698-2704.

Min, K.D. Kim, M.Y. Choi, K.Y. Lee, J.H. Lee, S.G., (2006). Effect of layered silicates on the crystallinity and mechanical properties of HDPE/MMT nanocomposite blown films. *Polymer Bulletin, 57*, 101-108.

Miyagawa, H., Rich, M. J., & Drzal, L. T. (2006). Thermo-physical properties of epoxy nanocomposite reinforced by carbon nanotubes and vapour grown carbon fibres. *Thermochimica Acta, 442*, 67-73.

Mohod, A.V., & Gogate, P.R. (2011). Ultrasonic degradation of polymers: Effect of operating parameters and intensification using additives for carboxymethyl cellulose (CMC) and polyvinyl alcohol (PVA). *Ultrasonics Sonochemistry, 18*, 727-734.

Montserrat, S., Calventus, Y., & Hutchinson, J. M. (2006). Physical aging of thermosetting powder coatings. *Progress in Organic Coatings, 55*, 35-42.

Mostafa, B.A., Assaad, F.F., & Attia, M., (2007). Rheological and electrical properties of Egyptian bentonite as a drilling mud. *Journal of Applied Polymer Science, 104*, 1496-1503.

Murray, H.H., (1988). Kaolin minerals; their genesis and occurrences. *Reviews in Mineralogy and Geochemistry, 19 (1)*, 67-89.

Mustafa S., Heru, A., Christianto, I., & Ozgur Y. (2006). The effect of chemical A mixtures and mineral additives on the properties of self-compacting mortars. *Cement and Concrete Composites*, 28, 432-440.

OMNI Laboratories Incorporation. (1998). Rosette morphology of pure smectite montmorillonite clay. *Electronic references.* Retrieved November 23, 2011, from http://webmineral.com/specimens/picshow.php?id=1285&target=Montmorillonite

Paluszkiewicz, C., Stodolak, E., Hasik, M., & Blazewicz M. (2011). FT-IR study of montmorillonite–chitosan nanocomposite materials. *Spectrochimica Acta Part A Molecular and Biomolecular Spectroscopy, 79*, 784-748.

Panuccio, M., Crea, F., Sorgonà, A., & Cacco, G. (2008). Adsorption of nutrients and cadmium by different minerals: Experimental studies and modelling. *Journal of Environmental Management, 88*, 890-898.

Peng, Z., & Kong, L.X. (2007). A thermal degradation mechanism of poly(vinyl alcohol)/ silica nanocomposites. *Polymer Degradation and Stability, 92*, 1061-1071.

Peng, Z., Kong, L.X., & Li, S.D. (2005). Thermal properties and morphology of a Poly (vinyl alcohol)/silica nanocomposite prepared with a self-assembled monolayer technique, *Journal of Applied Polymer Science, 96*, 1436-1442.

Peng, Z., Kong, L. X., Li, S. D., & Spiridonov, P. J. (2006). Poly (vinyl alcohol)/silica nanocomposites : Morphology and thermal degradation kinetics. *Journal of Nanoscience and Nanotechnology, 6*, 3934-3938.

Peprnicek, T., Duchet, J., Kovarova, L., Malac, J., Gerard, J.F., & Simonik, J. (2006) Poly (vinyl chloride)/clay nanocomposites: X-ray diffraction, thermal and rheological behaviour. *Polymer Degradation and Stability, 91*, 3322-3329.

Perrin, F. X., Nguyen, T. M. H., & Vernet, J. L. (2007). Kinetic analysis of isothermal and nonisothermal epoxy-amine cures by model-free isoconversional methods. *Macromolecular Chemistry and Physics, 208*, 718-729.

Rahman, W.A.W.A., Lee, T.S., & Rahmat, A.R. (2010). Thermal behaviour and interaction of cassava starch filled with glycerol plasticised polyvinyl alcohol blends. *Carbohydrate Polymers, 81*, 805-810.

Rahmat, A.R., Rahman, W.A.W.A., Lee, T.S., & Yussuf, A.A. (2009). Approaches to improve compatibility of starch filled polymer system: A review. *Material Science and Engineering C, 29*, 2370-2377.

Ramaraj, B. (2006). Modified poly(vinyl alcohol) and coconut shell powder composite films: Physico-mechanical, thermal properties, and swelling studies. *Polymer – Plastics Technology and Engineering 45 (11*), 1227-1231.

Ramis, X., Morancho, J.M., Cadento, A., Salla, J.M., & Fernandez – Francos, X. (2007). Effect of oxygen on the photopolymerization of a mixture of two dimethylcrylates. *Thermochimica Acta, 463*, 81-86.

Rastogi, S., Lippits, D. R., Hohne, G. W. H., Mezari, B., & Magusin, P. C. M. (2007). The role of the amorphous phase in melting of linear UHMW-PE; Implications for chain dynamics. *Journal of Physics Condensed Matter, 19*, AR 205122.

Ray, S., & Bousmina, M. (2005). Biodegradable polymers and their layered silicate nanocomposites: In greening the 21st century materials world. *Progress in Material Science,50 (8)*, 962–1079.

Ray, S., & Okamoto, M. (2003). Polymer/layered silicate nanocomposite: A review from preparation to processing. *Progress in Polymer Science, 28*, 1539-1641.

Rodriguez, J. G. I., Carreira, P., Garcia- Diez, A., Hui, D., Artiaga, R., & Liz-Marzan, L. M., (2007). Nanofiller effect on the glass trasition of a polyurethane. *Journal of Thermal Analysis and Calorimetry, 87*, 45-47.

Run, M. T., Song, H. Z., Yao, C. G., & Wang, Y.J. (2007). Crystal morphology and nonisothermal crystallization kinetics of short carbon fiber/poly (trimethylene terephtalate) composites. *Journal of Applied Polymer Science, 106*, 868-877.

Ryan, K. P., Cadek, M., Nicolosi, V., Blond, D., Ruether, M., & Armstrong, G. (2007). Carbon nanotubes for reinforcement of plastics? A case study with poly(vinyl alcohol). *Composites Science and Technology, 67,* 1640–1649.

Saha, B., & Ghoshal, A. K. (2007). Model-free kinetics analysis of decomposition of polyporylene over Al-MCM-41. *Thermochimica. Acta, 460*, 77-84.

Saiter. A, Couderc, H., & Grenet, J. (2007). Characterisation of structural relaxation phenomena in polymeric materials from thermal analysis investigations. *Journal of Thermal Analysis Calorimetry, 88*, 48-88.

Saltali, K., Sari, A., & Aydin, M. (2007). Removal of ammonium ion from aqueous solution by natural Turkish (Yıldızeli) zeolite for environmental quality. *Journal of Hazardous Materials, 141*, 258–263.

Samer Shaur Ali. (2010). Fundamental interactions and physical properties of starch, polyvinyl alcohol and montmorillonite clay based nanocomposites prepared using solution mixing and melt extrusion . A Master of Science thesis, Kansas state University, Manhattan

Sanchez-Valdes, S., Lopez-Quintanilla, M., Ramirez-Vargas, E., Francisco, J., Rodrıguez, J.M., & Gutierrez-Rodriguez., (2006). Effect of ionomeric compatibilizer on clay dispersion in Polyethylene/Clay nanocomposites. *Macromolecular Materials and Engineering, 29*1, 128-136.

Sargsyan, A., Torloyan, A., Davtyan, S., & Schick, C. (2007). The amount of immobilized polymer in PMMA SiO_2 nanocomposite determined from calorimetric data. *European Polymer Journal, 43,* 3113-3127.

Sbirrazzuoli, N., Mititelu-Mija, A., Vincent, L., & Alzina, C. (2006). Isoconversional kinetics analysis of stoichiometric and off-stoichiometic epoxy-amine cures. *Thermochimica Acta, 441*, 167-177.

Schlemmer, D., Angelica, R. S., Maria Jose., & Sales, R. S. (2010). Morphological and thermomechanical characterization of thermoplastic starch/montmorillonite nanocomposites. *Composite Structures, 92*, 2066-2070.

Sengwa, R.J., Choudhary, S., & Sankhla, S. (2009). Dielectric spectroscopy of hydrophilic polymers–montmorillonite clay nanocomposite aqueous colloidal suspension. *Colloids and Surfaces A: Physicochemical and Engineering Aspects, 336*, 79–87.

Selvakumara, V., Palanikumar, K., & Palanivelu, K. (2010). Studies on Mechanical Characterization of Polypropylene/Na+-MMT nanocomposites. *Journal of Minerals & Materials Characterization & Engineering, (9)*, 671-681.

Sender, C., Dantras- Laffont, I., Lacoste, M. H., Dandurand, J., Mauzac, M., Lacout, J. L., Lavergne, C., Demont, P., Bernes, A., & Lacabanne, C. (2007). Dynamic mechanical properties of a biomimetic hydroyapatite/polyamide 6’9 nanocomposite. *Journal of Biomedical Materials Research Part B: Applied Biomaterials, 83,* 628-635.

Shah, R.K., & Paul, D.R. (2006). Organoclay degradation in melt processed polyethylene nanocomposites. *Polymer, 147*, 4075-4084.

Shan, D., Zhu, M., Han, E., Xue, H., & Cosnier, S. (2007). Calcium carbonate nanoparticles: A host matrix for the construction of highly sensitive amperometric phenol biosensor. *Biosensor and Bioelectronics, 22*, 1612-1617.

Sharma, S.K., & Nayak, S.K., (2009). Surface modified clay/polypropylene (PP) nanocomposites: effect on physico-mechanical, thermal and morphological properties. Polymer Degradation and Stability, 94, 132-138.

Sharma, S.K., Nema, A.K., & Nayak, S.K. (2010). Polypropylene nanocomposite film: A critical evaluation on the effect of nanoclay on the mechanical, thermal, and morphological behaviour. *Journal of Applied Polymer Science, 115*, 3463-3473.

Siddaramaiah Raj, B., & Somashekar, R. (2004). Structure-property relation in polyvinyl alcohol/starch composites. *Journal of Applied Polymer Science, 91*, 630–635.

Silvestre, C., Cimmino, S., Duraccio, D., & Schick, C. (2007). Isothermal crystallization of isotactic poly (propylene) studied by superfast calorimetry. *Macromolecular Rapid Communications, 28*, 785-881.

Sin , L.T., Rahman, W.A.W.A., Rahmat, A.R., & Khan, M.I. (2009). Detection of synergistic interactions of polyvinyl alcohol-cassava starch blends through DSC. *Carbohydrate Polymers, 79*, 224-226.

Sin, L.T., Rahman, W.A.W.A., Rahmat, A.R., & Samad, A.A. (2010). Computational modelling and experimental infrared spectroscopy of hydrogen bonding interaction in polyvinyl alcohol-starch blends. *Polymer, 51*, 1206-1211.

Sin, L.T., Rahmat, A.R., Rahman, W.A.W.A., Sun, Z.Y., & Samad, A.A., (2010). Rheology and thermal transition state of polyvinyl alcohol-cassava starch blends. *Carbohydrate Polymers, 81*, 737-739.

Singhaa, N.R., Paryab, T.K., & Raya, S.K. (2009). Dehydration of 1,4-dioxane by pervaporation using filled and crosslinked polyvinyl alcohol membrane. *Journal of Membrane Science, 340*, 35-44.

Sinha, R. S., Bandyopadhyay, J., & Bousmina, M. (2007). Thermal and thermomechanical properties of poly[(butylene succinate)-co-adipate] nanocomposite. *Polymer Degradation and Stability,92 (5),* 802-812.

Sinha, R. S., & Bousmina, M. (2005). Biodegradable polymers and their layered silicate nanocomposites: In greening the 21st century materials world. *Progress in Materials Science, 50 (8),* 962-1079.

Sirousazar, M. Kokabia, M. Hassan, Z.M. Bahramiana, A.R., (2011). Dehydration kinetics of polyvinyl alcohol nanocomposite hydrogels containing Na-montmorillonite nanoclay. *Scientica Iranica Transactions F: Nanotechnology*.

Spiridon, Iuliana. Popescu, Maria Cristina. Bodarlau, Ruxanda. Vasile, Cornelia., (2008). Enzymatic degradation of some nanocomposites of poly(vinyl alcohol) with starch. *Polymer Degradation and Stability, 93*, 1884–1890.

Stoeffler, K., Lafleur, P.G., & Denault, J., (2008). Effect of intercalating agents on clay dispersion and thermal properties in polyethylene/montmorillonite nanocomposites. *Polymer Engineering and Science, 48*, 1449-1466.

Strawhecker, K. E., & Manias, E. (2000). Structure and properties of poly(vinyl alcohol)/Na+ montmorillonite nanocomposites. *Chemistry of Materials, 12(10)*, 2943–2949.

Su, J. F., Huang, Z., Liu, K., Fu, L. L., & Liu, H. R., (2007). Mechanical properties, biodegradation and water vapor permeability of blend films of soy protein isolate and poly (vinyl alcohol) compatibilized by glycerol. *Industrial Crops and Products,(31).*266-276.

Suleiman, D., Napadensky, E., Sloan, J. M., & Crawford, D. M. (2007). Thermogravemetric characterization of highly sufonated poly (styrene-isobutylene-styrene) block copolymers : Effect of sulfonation and counter-ion substitution surface charge. *Thermochimica Acta, 460*, 35-40.

Szep, A. Szabo, A. Toth, N. Anna, P. Marosi G., (2006). Role of montmorillonite in flame retardancy of ethylene–vinyl acetate copolymer. *Polymer Degradation and Stability, 91*, 193-197.

Taghizadeh, M.T., & Abbasi, Z. (2010). Enzymatic degradation of starch/PVA composite film containing Montmorillonite nanoparticle. The 13th Asia Pacific Confederation of Chemical Engineering Congress, Taipei.

Takegawa, K., Fukao, K., & Saruyama, Y. (2007). Aging effect on thermal expansion coefficient and the heat capacity of glassy polystyrene studied with simultaneous measurement using temperature modulation technique. *Thermochimica Acta, 461*, 67-71.

Tang, S., Zou, P., Xiong, H., & Tang, H. (2005). Effect of nano-SiO2 on the performance of starch/polyvinyl alcohol blend films. *Carbohydrate Polymers, 72*, 521–526.

Tang, X., & Alavi, S. (2011). Review : Recent advances in starch, polyvinyl alcohol based polymer blends, nanocomposites and their biodegradability. *Carbohydrate Polymers, 85*,7-16.

Tang, Y., Hu, Y., Song, L,. Zong, R., Gui, Z., Chen, Z., & Fan, W. (2003). Preparation and thermal stability of polypropylene/ montmorillonite nanocomposites. *Polymer Degradation and Stability, 82*, 127-131.

Thakore, I.M., Desai, S., Sarawade, B.D. & Devi, S. (2001). Studies on biodegradability, morphology and thermomechanical properties of LDPE/modified starch blends. *European Polymer Journal, 37 (1),* 151-160.

Tidjani, A., & Wilkie, C. A. (2006). TGA analysis of γ-irradiated linear low-density polyethylene. *Journal of Applied Polymer Science, 100*, 2790-2795.

Tjong,,S. (2006). Structural and mechanical properties of polymer nanocomposites. *Material Science and Engineering ,53*, 73-197.

Trujillo, M., Arnal, M. L., Mueller, A. J., Laredo, E., Bredeau, St., Bonduel, D., & Dubios, Ph. (2007). Thermal and morphological characterization of nanocomposites prepared by in-site polymerization of high-density polyethylene on carbon nanotubes. *Macromolecules, 40*, 6268-6276.

Tudorachi, N., Cascaval, C.N., Rusu, M., & Pruteanu, M. (2000). Testing of polyvinyl alcohol and starch mixtures as biodegradable polymeric materials. *Polymer Testing, 19 (7)*, 785-799.

Tunc, S., & Duman, O. (2010). Preparation and characterization of biodegradable methyl cellulose/montmorillonite nanocomposite films. *Applied Clay Science, 48,* 414-424.

Tunc, S., & Duman, O. (2011). Preparation of active antimicrobial methyl cellulose/carvacrol/montmorillonite nanocomposite films and investigation of carvacrol release. *Food Science and Technology, 44*, 465-472.

Vaccari, A. (1999). Clays and catalysis: A promising future. *Applied Clay Science, 14*, 161-198.

Van Jaarsveld JGS., Van Deventer JSJ., & Lorenzen L. (1997). The potential use of geopolymeric materials to immobilise toxic metals: Part I. Theory an applications. *Mineral Engineering, 10*, 659-669.

Vasile, C., Stoleriu, A., Popescu, M. C., Duncianu, C., Kelnar, I., & Dimonie, D. (2008). Morphology and thermal properties of some green starch/poly (vinyl alcohol)/montmorillonite nanocomposites. *Cellulose Chemistry and Technology, 42(9–10)*, 549–568.

Vasko, P. D., Blakwell, J., & Koening, J. L., (1972). Infrared and Raman spectroscopy of carbohydrates. 2. Normal coordinate analysis. *Carbohydrate Research, 23*, 407-416.

Viviana P. Cyras., Liliana B., Manfredi, Minh-Tan Ton-That., & Analia Vazquez. (2008). Physical and mechanical properties of thermoplastic starch/montmorillonite nanocomposite films. *Carbohydrate Polymers, 73*, 55-63.

Wu, Bo., Qi, Shuhua., & Wang, Xin. (2010). Thermal behaviour of poly(vinyl chloride) treated with montmorillonite-silica-3-triethoxysilyl-1-propanamine (K-Si-MMT) nanocomposite. *Polymer Testing, 29*, 717-722.

Xi, Y., Martens, W., He, H., & Frost, R.L. (2005). Thermogravimetric analysis of organoclays intercalated with the surfactant octadecyltrimethylammonium bromide. *Journal of Thermal Analysis and Calorimetry, 81*, 91-97.

Xie, W., Gao, Z., Pan, W.-P., Hunter, D., Singh, A., & Vaia, R. (2001). Thermal degradation chemistry of alkyl quaternary ammonium montmorillonite. *Chemistry of Materials, 13*, 2979-2990.

Xie, W., Xie, R., Pan, W.-P., Hunter, D., Koene, B., Tan, L.-S., & Vaia, R. (2002). Thermal stability of quaternary phosphonium modified montmorillonites. *Chemistry of Materials, 13, 9*, 2979-2990.

Xiong, J., Zheng, Z., Jiang, H., Ye, S., & Wang, X. (2007). Reinforcement of polyurethane composites with an organically modified montmorillonite. *Composites Part A: Applied Science and Manufacturing, 38*, 132-137.

Xu, H., & Van Deventer JSJ. (2000).The geopolymerisation of aluminosilicate minerals. *International Journal of Mineral Processing, 59*, 247-266.

Zenggang, W., Chixing, Z., & Na, Z. (2002). The nucleating effect of montmorillonite on crystallization of nylon 1212/montmorillonite nanocomposite. *Polymer Testing, 21*, 479-483.

Zhang, D., Tong, D.S., Xia, H.S., Jiang, G.F., Xia, X., Liu, M., Yu, W.H., & Zhou, C.H. (2009). Hydrothermal synthesis of clay minerals.14th Intl. Clay Conf, Micro ET Nano ScientlE Mare Magnum, Castellaneta M, Italy, p.432.

Zhang, D., Zhou, C.H., Lin, C.X., Tong, D.S., & Yu, W.H. (2010). Review Paper Synthesis of clay minerals. *Applied Clay Science, 50 (1),* 1-11.

Zhang, G. Ding, P. Zhang, M. & Qu, B. (2007). Synergistic effects of layered double hydroxide with hyperfine magnesium hydroxide in halogen-free flame retardant EVA/HFMH/LDH nanocomposites. Polymer Degradation and Stability, 92, 1715-1720.

Zhang, M., Ding, P., Du, L., & Qu, B. (2008). Structural characterization and related properties of EVA/ZnAl-LDH nanocomposites prepared by melt and solution intercalation. *Materials Chemistry and Physics, 109*, 206-211.

Zhao, C., Qin, H., Gong, F., Feng, M., Zhang, S., & Yang, M. (2005). Mechanical, thermal and flammability properties of polyethylene/clay nanocomposites. *Polymer Degradation and Stability, 87*, 183-189.

Zhou, C.H. (2010). Emerging trends and challenges in synthetic clay-based materials and layered double hydroxides. *Applied Clay Science, 48 (1-2),* 1-4.

Zhou, C.H., Du, Z.X., Li, X.N., Lu, C.S., & Ge, Z.H. (2005). Structure development of hectorite in hydrothermal crystallization synthesis process. *Journal of Inorganic Chemistry, 21 (9),* 1327-1332.

Zhu, L., Letaief, S., Liu, Y., Gervais, F., & Detellier, C. (2009). Clay mineral-supported gold nanoparticles. *Applied Clay Science, 43,* 439-446.

Zong, R., Hua, Y., Wanga, S ,.& Songa, L. (2004). Thermogravimetric evaluation of PC/ABS/montmorillonite nanocomposite. *Polymer Degradation and Stability*, 83, 423-428.

APPENDICES

APPENDIX A: Graphs